From a coastal plain to an anthropized fluvial valley (NW Brittany, France): 7.3 kyr of paleoenvironmental evolution from sedimentological, palynological and paleogenomic perspectives

Ophélie David, Muriel Vidal, Aneta Gorczyńska, Aurélie Penaud, Yvan Pailler, Clement Nicolas, Evelyne Goubert, Pierre Stéphan, Morgane Ollivier, Frédérique Barloy-Hubler

Quaternary Science Reviews 344 (2024) 108983

Contents lists available at ScienceDirect

Quaternary Science Reviews

journal homepage: www.elsevier.com/locate/quascirev

From a coastal plain to an anthropized fluvial valley (NW Brittany, France): 7.3 kyr of paleoenvironmental evolution from sedimentological, palynological and paleogenomic perspectives

Ophélie David [a,b,*], Muriel Vidal [a], Aneta Gorczyńska [c], Aurélie Penaud [a], Yvan Pailler [c], Clément Nicolas [d], Evelyne Goubert [b], Pierre Stéphan [c], Morgane Ollivier [e,1], Frédérique Barloy-Hubler [e,1]

[a] Geo-Ocean, UMR 6538, Univ Brest, CNRS, Ifremer, F-29280, Plouzané, France
[b] Geo-Ocean, UMR 6538, Univ Bretagne Sud, Univ Brest, CNRS, Ifremer, F-56000, Vannes, France
[c] LETG, UMR 6554, CNRS, Univ Brest, Nantes Univ, Univ Rennes 2, IUEM, F-29280, Plouzané, France
[d] Trajectoires, UMR 8215, CNRS, Univ Paris-1Panthéon Sorbonne, F-75105, Paris, France
[e] ECOBIO, UMR 6553, Univ Rennes 1, CNRS, F-35042, Rennes, France

ARTICLE INFO

Handling editor: P Rioual

Keywords:
Holocene
Western Europe
Neolithic
Bronze Age
Iron Age
Pollen grains
Ancient sedimentary DNA (sedaDNA)
Paleoenvironmental changes
Agropastoral activities

ABSTRACT

Over the Holocene (last 11.7 kyr), the Brittany coastal region has undergone major changes in response to rising sea level, climatic fluctuations and increasing anthropogenic influence. This study aims to i) accurately reconstruct the paleoenvironmental evolution of a site located on the north Brittany coast (NW France), a sector that has not been previously investigated thoroughly, and ii) improve the detection of the anthropogenic signature in paleoenvironmental records by using a multidisciplinary approach. To achieve these goals, we made the first cross-correlated study in coastal Brittany region, integrating sedimentological (grain-size, X-ray fluorescence), palynological (pollen grains), and paleogenomic (on plant and mammal sedimentary ancient DNA or sedaDNA) data, which we based two 7.3 kyr-long sedimentary sequences recovered from the Kerallé valley (Plouescat, NW Brittany).

First, sedimentary and vegetation trajectories allowed us to reconstruct the evolution of past depositional environments in the inner part of the Kerallé valley. The data show a progressive sedimentary infilling of the former alluvial plain, subjected to marine incursion between 7.3 and 6 cal ka BP, up to a continental area, totally disconnected from tidal influence since 5.4 cal ka BP. Second, the analysis of plant and mammal sedaDNA provided a complementary tool to the pollen analysis, enhancing our ability to accurately detect past land-use practices. In the upstream part of the Kerallé system, anthropogenic influence remained scarce until the late Neolithic and seemed to be restricted to the coast, as also indicated by archaeological remains. The first significant human-driven changes in plant community composition likely date back to 4.5 cal ka BP (i.e., late Neolithic), as also shown by the presence of domesticated mammal sedaDNA, both being in agreement with the documented settlement by the first metal-working societies (Bell Beaker culture) in the Plouescat area. From then until 4 cal ka BP (i.e., early Bronze Age), human pressure became more obvious, with the steadily increase in anthropogenic pollen indicators, while sedaDNA of plants and mammals were affected by preservation biases. At 2.7 cal ka BP (i.e., Iron Age), a new anthropic threshold was characterized by maximal forest clearing leading to significant human-induced soil erosion across the Kerallé watershed. Since then, at the local scale of our study, both vegetation dynamics and the presence of domesticated mammals observed by sedaDNA attest to the development of pastoralism.

* Corresponding author. Geo-Ocean, UMR 6538, Univ Brest, CNRS, Ifremer, F-29280, Plouzané, France.
E-mail address: ophelie.david@univ-brest.fr (O. David).
[1] Contributed equally.

https://doi.org/10.1016/j.quascirev.2024.108983
Received 3 May 2024; Received in revised form 19 September 2024; Accepted 20 September 2024
Available online 10 October 2024

1. Introduction

Since the deglaciation, the Holocene (i.e., last 11.7 kyr) has been characterized by the rise of the Relative Sea Level (RSL; e.g., Atlantic coasts: Leorri et al., 2012a, b; García-Artola et al., 2018) affecting coastal geomorphological evolution and sedimentary fluxes (e.g., Stéphan, 2019). Coastal zones have therefore undergone perpetual changes under the influence of interlinked mechanisms operating on global- to local-scale, including RSL rise, sedimentary fluxes as well as natural climatic fluctuations operating at different sub-orbital timescales (Bond et al., 1997, 2001; Mayewski et al., 2004). At the scale of the western Brittany coasts (NW France), the early Holocene period (i.e., 11.7 to 8.2 cal ka BP) was characterized by high RSL rise rates (~9 mm/yr; from −40 to −12 m) that subsequently slowed down from ~7 to 6 cal ka BP (~1 mm/yr; García-Artola et al., 2018). Superimposed on these natural forcings, the anthropogenic influence on the environment grew as profound cultural and technical changes took place, such as the settlement of the first agro-pastoral communities during the Neolithic period (i.e., 7–4.2 cal ka BP in Brittany; e.g., Cassen et al., 1998; Pailler, 2007; Pailler et al., 2008; Tinévez et al., 2015; Juhel et al., 2015; Marchand, 2021) or the development of metal-working societies during the Bronze and Iron Ages (4.2–2.7 and 2.7–2 cal ka BP, respectively; e.g., Briard, 1984; Giot et al., 1995; Menez and Lorho, 2013; Daire et al., 2015; Blanchet et al., 2017, 2019; Gandini, 2022).

The first pollen studies in Brittany, conducted on continental peat bogs, i.e., time-restricted sedimentary archives (e.g., van Zeist, 1963; Morzadec-Kerfourn, 1974; Marguerie, 1992; Visset et al., 1995, 1996) made it possible to depict changes in long-term Holocene vegetation cover thanks to the stacking of several pollen spectra (Gaudin, 2004; David, 2014). The study of mid-shelf continuous sequences collected on the northwestern French margin (Naughton et al., 2007; Lambert et al., 2019; Penaud et al., 2020; David et al., 2022), has then highlighted the interconnexion of long-term (orbital) and short-term (millennial) Holocene climate variability. Acting at different spatio-temporal timescales, the forcings mainly include the impact of RSL rise, fluctuating river discharges under subpolar gyre strength modulation and related precipitation regime fluctuation, as well as sedimentary fluxes. These studies show how anthropogenic impact on western France and southern Brittany watersheds has increased through the Holocene, with major regional thresholds discussed at ~4.2 cal ka BP (i.e., start of the Bronze Age) and ~1.2 cal ka BP (i.e., start of the Middle Ages; Naughton et al., 2007; Lambert et al., 2019; Penaud et al., 2020; David et al., 2022). At a more local scale, coastal sedimentary sequences covering the last 7 kyr allowed reconstruction of relationships between climate variations, vegetation dynamics, and early human activities in western (Fernane et al., 2014) and southern (Fernane et al., 2015) Brittany. However, to date, no continuous long-term archive exists to allow the reconstruction of northern Brittany paleoenvironments, as the temporal scope of the studies in Morzadec-Kerfourn (1974) was limited. The present multiproxy study therefore aims to fill this gap over the last 7.3 kyr, based on long-term and stratigraphically continuous sediment sequence collected on the north Finistère coast (core ANE-C3), in the inner part of the Kerallé valley (Plouescat, NW Brittany, France).

It is generally accepted that increases of Anthropogenic Pollen Indicators (API) in pollen spectra, including ruderals, arable weed species and cultivated taxa, are associated with human-induced impacts on watersheds adjacent to the coring sites (e.g., Behre, 1981; Marguerie, 1992; Mazier et al., 2006). Their occurrences are usually associated with a drop in arboreal taxa percentages, indicating increasing deforestation. However, the detection and interpretation of API in coastal sediments are still challenging (e.g., Lambert et al., 2017; David et al., 2022) due to ecological variations (e.g., low pollen production by some entomophilous API taxa, and effects of pollination season) and taphonomic issues (e.g., transport under fluvial discharges or preservation, which vary according to sedimentary basin and fluxes). Indeed, coastal environments become reorganized under RSL rise, with more or less marine influence, making them suitable for specific halophilous species that are congeneric with some API. The low taxonomic resolution of some herbaceous pollen grains prevents us from discriminating among members of the same family, and therefore between species that occur in anthropized environments and those growing naturally in coastal environments (e.g., in Amaranthaceae family, *Chenopodium album* versus *Halimione portulacoides*).

Over the last two decades, ancient sedimentary DNA (sedaDNA) has therefore usefully complemented studies on pollen and macro-remains, proving valuable for studying past landscape trajectories and agro-pastoral practices (e.g., Hebsgaard et al., 2009; Giguet-Covex et al., 2014; Parducci et al., 2019; Messager et al., 2022; Hudson et al., 2022). To date, however, no such studies have been performed in a northwestern European coastal context. In addition, X-ray fluorescence (XRF) analysis, provides elemental geochemistry data, often used to trace sediment origin (e.g., terrigenous vs. biogenic), and has demonstrated its value in different sedimentary contexts to reconstruct Holocene paleoenvironmental history in combination with other proxies (e.g., continental archives: Brisset et al., 2013; Bajard et al., 2016; Mensing et al., 2015 / estuarine archive: Durand et al., 2018 / marine archive: Penaud et al., 2020). For these reasons, we performed analyses on twin cores from the same site, retrieved within a 10–15 m of one another: the ANE-C3 core, used for palynological and geochemical (XRF) analyses, and the PADMé core, used for sedaDNA data analysis. Cross-correlation was therefore possible between the cores and the multiproxy approach allows us to discuss land use practices more accurately through a comprehensive analysis of spatial and temporal patterns of environmental variations and species dynamics, from the Mesolithic to the Roman period.

2. Environmental and archaeological contexts

2.1. Geomorphological context of the bay of Goulven and Kerallé valley

Located in northwest Brittany (NW France), the study area of Plouescat is crossed by the Kerallé valley that flows into the bay of Goulven, extending from Brignogan to Plouescat (Fig. 1a and b). This bay is located at the transition between the Léon platform (with metamorphic rocks inherited from the Variscan orogeny) and the submarine plain of *La Manche* (or English Channel; Battistini, 1953, Fig. 1a). The contact between these continental and coastal domains corresponds to a tectonic paleo-escarpment 40–50 m high (Battistini and Martin, 1956; Stéphan et al., 2018; paleocliffs in Fig. 1c). A gentle slope marks the transition between the intertidal zone and deeper environment, up to 50 m deep (Battistini and Martin, 1956). This configuration was produced by the erosive action of previous high sea-level stagnation and of the fluvial system which is made up of five tributaries (la Flèche, le Frout, ar Rest, Kerrus and Kerallé rivers; Fig. 1c) that have shaped the marine platform over 25 km (Battistini, 1953, 1955; Battistini and Martin, 1956).

Along the coast, the exposed granitic rocks are deeply eroded and overlain by Quaternary deposits. In addition, rocky outcrops have allowed the anchoring of sand deposits and development of the current coastal dune system known as the Keremma system, extending over 7 km (Fig. 1c; Hallégouët and Moign, 1976; Menez, 1977; Yoni and Hallégouët, 1998; Stéphan et al., 2018). Archaeological artefacts collected within this dune complex indicate dune establishment at around 450 cal a BP (Gorczyńska et al., 2023a, 2023b). In the eastern part, the dune evolved into a sandy spit prograding eastward and partially closing off Kernic Cove (Fig. 1c).

Kernic Cove is drained by a channel fed by three main tributaries: the Ar Rest, Kerrus and Kerallé rivers. This system forms the Kerallé valley, with a watershed extending over 70 km^2 (Fig. 1b). Connected to *La Manche*, the Kerallé valley and more broadly the bay of Goulven have evolved profoundly during the Holocene due to the global Relative Sea Level (RSL) rise.

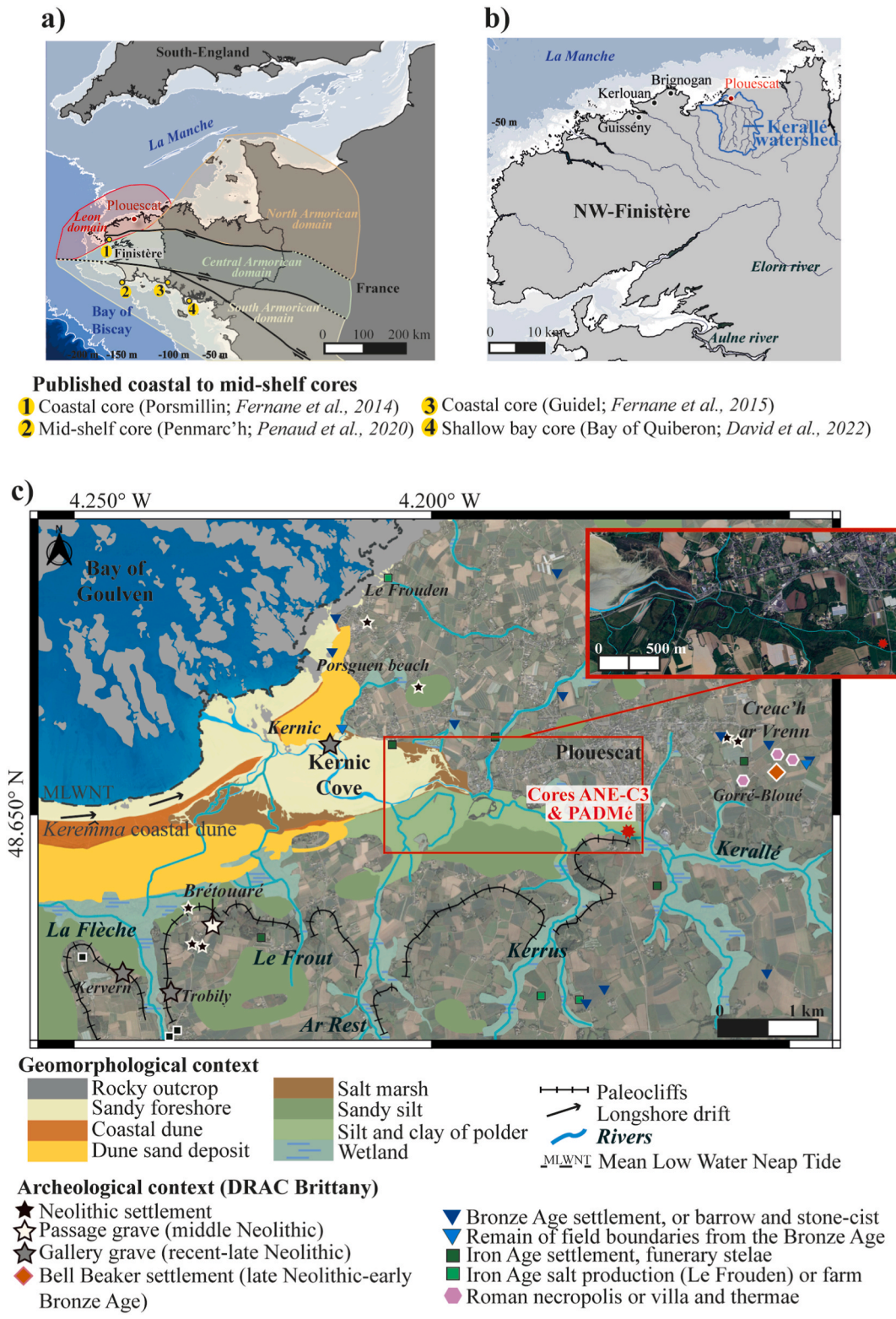

Fig. 1. Location of a) the Finistère region in northwestern France and major geological domains of the Armorican Massif (according to *Ballèvre* et al., *2013*), and b) Kerallé watershed and Plouescat in north Finistère. c) Sedimentological and geomorphological map of the downstream part of Kerallé valley (modified from *Hallégouët and Moign, 1976*; *Stéphan* et al., *2018*) showing the locations of the studied cores (ANE-C3 and PADMé) and the main archaeological monuments (from the DRAC-GeoBretagne).

2.2. Relative sea level (RSL) evolution and implications for the Brittany coastal landscape

Paleocliffs outlining the edge of the Léon platform, which can be observed along the bay of Goulven coastline (Fig. 1c), correspond to marine cliffs whose dating is uncertain but which testify to an earlier period of elevated sea level (~20 m above the current sea level; Giot et al., 1965; Hallégouët and Moign, 1976).

The Holocene transgression along the European coasts has been extensively studied and quantified thanks to sedimentological archives (e.g., Lambeck et al., 1998; Brooks and Edwards, 2006; Leorri et al., 2012a, b; García-Artola et al., 2018). Archaeological remains are also good indicators of RSL rise with numerous megalithic monuments currently found in intertidal and subtidal domains along Brittany's coasts (e.g., Devoir, 1912; Giot and Morzadec, 1992; Baltzer et al., 2015). Around the bay of Goulven, the Kernic gallery grave (located on the foreshore of Kernic Cove; Fig. 1c; Lecerf, 1985; Gorczyńska et al., 2023b) partially submerged during high spring tides, testifies to the last rise of RSL, since its construction dates back to the recent to late Neolithic (i.e., ~5.3–4.2 ka BP). During the early Holocene (11.7–8.2 cal ka BP), the RSL rise rates were very high (~9 mm/yr along the western Brittany coast; García-Artola et al., 2018) before decreasing during the middle Holocene (~1 mm/yr). Along western Brittany coasts, the slowdown of the RSL rise was indeed recorded at around 7–6 cal ka BP (Goslin et al., 2015; Stéphan et al., 2015; García-Artola et al., 2018), and allowed the development of the modern coastline, with salt marshes or freshwater marshes behind coastal barriers (Morzadec-Kerfourn, 1974; Goslin et al., 2013; Stéphan et al., 2015). Moreover, in estuarine environments, this RSL rise inflexion allowed the stabilization of riverbanks and fluvial valley alluviation responsible for the development of the riparian forest at around 6 cal ka BP (Penaud et al., 2020; David et al., 2022).

2.3. Cultural and archaeological evidence around the bay of Goulven

Evidence of human occupation during the second Mesolithic is scarce around the bay of Goulven, both inland and on the Léon plateau, with only two sites yielding a few armatures typical of this period (Pailler, 2007). Similarly, the early Neolithic is represented by ring-shaped stones attesting that the sector was visited by human groups. Indeed, the concentration of archaeological remains represented mainly by megalithic graves in this area, increased through the Neolithic period (Lecerf, 1983, 1984; Sparfel et al., 2004; Gorczyńska et al., 2023b). The Brétouaré passage grave (Fig. 1c), constructed during the middle Neolithic (~6.2 and 5.7 cal ka BP/~4.3–3.8 ka BCE), is the oldest and only known monument around the bay of Goulven, although this type of monument is highly concentrated along the northwestern coast of Finistère (Sparfel et al., 2004; Sparfel and Pailler, 2009). Middle to Recent Neolithic settlements are still lacking close to the study area but, a little further westward, evidence of settlement has been identified in coastal peat bogs in the NW Brittany foreshore (e.g., Curnic in Guissény, Giot et al., 1965; Tréssény in Kerlouan, Hallégouët et al., 1971, Fig. 1c), suggesting that human groups were settling on the coastal plain. Then, the recent and late Neolithic periods are marked by the development of gallery graves (5.3–4.5 cal ka BP/3.3–2.5 ka BCE), found across a broad geographical range and extending from coastal to inland areas. The construction of at least 8 gallery graves around the bay of Goulven suggests an important settlement dynamic (Sparfel, 2002; Sparfel et al., 2004; Gorczyńska et al., 2023b; 3 graves are indicated in Fig. 1c). For the subsequent period (4.5–4.2 ka BP/2.5–2.2 ka BCE), the discovery of inland Bell Beaker settlements at Creac'h ar Vrenn (Nicolas et al., 2015, Fig. 1c) testifies to a persisting human occupation. The Bell Beaker culture is known to have spread out in Brittany at the transition between the late Neolithic and early Bronze Age (i.e., 4.5–3.9 cal ka BP; Nicolas, 2016a; Nicolas et al., 2019). The early Bronze Age (4.2–2.7 cal ka BP/2.2–0.7 ka BCE) in Plouescat is then well documented with barrows, stone-cists, and remains of field boundaries beyond the Kernic gallery grave (Lecerf, 1985) and possibly at Creac'h ar Vrenn (Nicolas et al., 2015, Fig. 1c). In particular, we should mention the old discovery of a barrow yielding 22 finely-shaped arrowheads and a bronze dagger, symbols of the early Bronze Age elite (4–3.8 cal ka BP/2–1.8 ka BCE), at 1.5 km south of the coring site (Nicolas, 2016b). In this anthropized environment, pastoral activities are attested by the discovery of domestic mammal bones (i.e., *Bos* ssp., *Ovis* ssp. and *Equus* spp.; Briard et al., 1970) and numerous sherds, attributed to the early-middle Bronze Age (*Pailler, pers. comm.*) within a peat bog layer located at Porsguen beach (Fig. 1c). Around the bay of Goulven, numerous funerary stelae and souterrains attributed to the Iron Age (2.7–2 cal ka BP/75–50 BCE) are commonly found (e.g., Le Goffic, 2002a, b; Villard-Le Tiec, 2011; Bossard, 2015). In Brittany, these types of remains are associated with farms (e.g., Villard-Le Tiec, 2011; Menez and Lorho, 2013; Bossard, 2015). Around the bay of Goulven, there was also a settlement specialized in the sea salt production (Le Frouden; Le Goff and Roué, 1991; Daire et al., 2015, Fig. 1c). The construction of a villa and thermae close to the Kerallé valley (Gorré-Bloué; Abgrall, 1919; Gandini, 2022, Fig. 1c) testifies to a substantial and continuous occupation over the Roman period (i.e., 2–1.6 cal ka BP/50 BCE–350 CE). During the Middle Ages (not examined in this study) economic practices and demographics continued to grow and human imprint on environment became increasingly predominant through territorial reorganization and the development of agrarian landscape throughout Brittany (Marguerie, 1992; Fernane et al., 2015).

3. Materials and methods

3.1. General information on study sediment cores and AMS-^{14}C dating

Core ANE-C3 (48°38′54.5114″N; 4°10′21.3848″W; 12 m long) was retrieved in 2018 from the current wetland of the Kerallé river, Plouescat (Fig. 1c), with a Cobra (Eikjelkamp) percussion corer. For this core, 19 AMS-^{14}C dates (Table 1) were acquired on bulk (5 samples) and on plant macro-remains (14 samples). In 2021, on the same site (within a 10–15 m radius), a twin core, called PADMé, was retrieved (same geographic coordinates, 10 m long), again with the Cobra percussion corer. For core PADMé, 8 AMS-^{14}C were acquired (Table 2) on organic sediments (4 samples) and on plant macro-remains (4 samples).

All radiocarbon dates were calibrated with CALIB 7.1 software, using the IntCal20 calibration curve (Stuiver and Reimer, 1993; Reimer et al., 2020). The final age models of both cores (Figs. 2 and 3a) were established using the rbacon package (Blaauw and Christen, 2011) in R version 4.12 (R Development Core Team, 2021; http://www.r-project.org/).

3.2. Sedimentological analyses

A detailed visual description of the sedimentary facies was performed on both cores. Grain size analyses, after removal of organic matter by H_2O_2 addition, were carried out using a Malvern Mastersizer 2000 laser diffractometer. These analyses were performed every ~10 cm along core ANE-C3 (116 samples), and every ~10–20 cm along core PADMé (45 samples). Grain size parameters (i.e., median grain size-D50, Figs. 2b and 3) were calculated using GRADISTAT v8.0 software (Blott and Pye, 2001).

Additional analyses were conducted on the ANE-C3 core. Measurement of total organic carbon (TOC%) and carbonate content ($CaCO_3$%) were performed (Fig. 2b) every 2 cm, using the standard Loss On Ignition (LOI) method (Heiri et al., 2001). Sediments were dried at 105 °C for 16 h, before being cooled in a desiccator. After weighing, samples were burned at 550 °C for 4 h and weighed to calculate the TOC. Finally, samples were burned at 950 °C for 2 h and weighed to calculate the carbonate content. X-ray fluorescence (XRF) analyses were performed using an "Avaatech core-scanning" device, with a 1-cm-step, to make semi-quantitative measurements of the major elements. A Canonical Correspondence Analysis (CCA) was performed on the geochemical results using the PAST program v4.03 (Hammer et al., 2001) to calculate statistical correlations between element variations (Fig. 2c). XRF data were then normalized using anti-correlated elements.

Table 1
List of all AMS-^{14}C dates obtained on core ANE-C3 (text in grey italics is modern date rejected for the age model).

Lab. Code	Depth (cm)	Dated material	Age ^{14}C a BP	± error	Age (cal a BP)		
					min	mean	max
Beta - 573652	*50.5*	*Fine rootlets*	*101.38 pMC*	*30*			
SacA-55035	86.5	Bulk	1670	30	1530	**1559.5**	1589
Beta - 573653	150	Fine rootlets	1880	30	1714	**1777**	1840
SacA −55043	212.5	Bulk	2610	30	2735	**2745**	2755
Beta - 570606	216.5	Fine rootlets	1690	30	1528	**1576**	1624
SacA-55044	267.5	Bulk	2380	30	2347	**2388**	2429
SacA-55039	354	Fine rootlets	2790	30	2852	**2894**	2936
Beta - 570607	395.5	Fine rootlets	2940	30	3060	**3111.5**	3163
SacA-55038	458.5	Fine rootlets	3035	30	3158	**3255**	3352
Beta - 570608	495	Fine rootlets	4100	30	4527	**4574**	4621
SacA-55042	527.5	Bulk	4040	30	4419	**4500**	4581
SacA-55037	665.5	Fine rootlets	4805	30	5482	**5504.5**	5527
SacA-55036	774.5	Plants	5275	30	5987	**6054**	6121
SacA-55041	872.5	Plants	5760	30	6485	**6570.5**	6656
SacA-55040	974.5	Bulk	6265	30	7156	**7210**	7264
SacA-55052	1058.5	Fine rootlets	6235	30	7013	**7070**	7127
SacA-55045	1078.5	Plants	6245	35	7154	**7205.5**	7257
SacA-55053	1094.5	Fine rootlets	6455	30	7314	**7370.5**	7427
SacA-55058	1128.5	Fine rootlets	6340	35	7252	**7230.5**	7209

Table 2
List of all AMS-^{14}C dates obtained on core PADMé (text in grey italics is a date rejected as inconsistent with all the others).

Lab. Code	Depth (cm)	Dated material	Age ^{14}C a BP	± error	Age (cal a BP)		
					min	mean	max
Beta-603598	85.5	Bulk	1530	30	1356	**1384.5**	1413
Beta-607886	255	Plants	2190	30	2114	**2215.5**	2317
SacA65348	359.5	Bulk	2840	30	2865	**2936.5**	3008
Beta-603600	*454.25*	*Plants*	*940*	*30*	782	***851.5***	921
Beta-603601	520	Bulk	3630	30	3895	**3937.5**	3980
Beta-603602	679.5	Plants	4340	30	4843	**4908.5**	4974
SacA65348	849.75	Plants	5180	30	5901	**5948.5**	5996
Beta-603603	991.75	Bulk	6320	30	7169	**7189.5**	7210

3.3. Palynological analyses on core ANE-C3

Pollen analyses were performed on 1 cm^3 sub-samples every 10–20 cm (i.e., 66 levels in total) making it possible to obtain an average 90-year time resolution. Pollen extraction on the <150 μm sediment fraction was carried out at the EPOC Laboratory (Univ. Bordeaux) following the procedure described by de Vernal et al. (1999). Chemical (cold 10% HCl and 40–70% HF) and physical (sieving with a 10-μm nylon mesh) treatments were performed to remove the mineral fraction and concentrate palynomorphs. Pollen determination was done on a Leica DMC 2900 optical microscope at ×630 magnification, using Beug (1961) and Reille (1995) for identification. To ensure statistical reliability, a minimum of 300 pollen grains were counted in each sample, excluding the largely dominant taxa *Alnus* and *Corylus* (each reaching 32% on average over the whole sequence). This threshold was not reached for only two levels (845 and 785 cm, where 215 and 140 pollens grains were counted, respectively; marked with an asterisk in Fig. 4).

For each level, Non-Pollen Palynomorphs (NPPs), mainly foraminiferal linings and dinoflagellate cysts (dinocysts), were counted. A total of 11 dinocyst species were identified, which correspond to shallow bays or inner-to-outer neritic domains according to the modern distribution described in Penaud et al. (2020) along the south-Armorican shelf. The percentages of NPPs were calculated on a sum including all palynomorphs identified in the palynofacies (i.e., pollen, spores, foraminifera and dinocysts; Fig. 4a).

Pollen percentages were calculated on a sum of pollen excluding indeterminate and local taxa (Cyperaceae, aquatic taxa and riparian trees mainly represented by *Alnus*). A pollen diagram was created using the Psimpoll program (Bennet, 1992), which also allows the definition of pollen zonation (named P) based on a stratigraphically constrained cluster analysis (CONISS; Grimm, 1987). Pollen zonations were confirmed (Fig. 4c) by a cluster analysis performed on the pollen percentages (with the Bray-Curtis similarity measure; Fig. 5) using the Past program v 4.03 (Hammer et al., 2001), also used to calculate ecological indexes (i.e., diversity: number of taxa per sample or Margalef index; and dominance; Fig. 4b).

To better characterize the anthropogenic influence, pollen grains were summed according to their ecological affinities (Rivière, 2007; Quéré et al., 2008). To define a list of anthropogenic pollen indicators, we carried out a literature review (e.g., Behre, 1981; Brun, 2011; Mazier et al., 2006; Marguerie, 1992) and a study of various pollen assemblages of the modern pollinic signal in the coastal environment of Plouescat (see Data in Brief for a calibration of the anthropogenic pollen signal around Kernic Cove, David et al., *submitted*). We thus defined two main anthropogenic pollen groups. The first of these indicators is the sum of ruderal and arable weed taxa that can develop in various anthropized environments, including: *Rumex acetosa*-type, *Polygonum aviculare, Polygonum nigra*, *Centaurea cyanus,* Urticaceae, and *Trifolium*. The second indicator is a separate representation of Pastoral Indicators (PI) including Asteroideae, Cichorioideae, and *Plantago lanceolata*, classically found in grazing areas (e.g., in Europe: Behre, 1986; Norway: Hjelle, 1999; Italy: Florenzano, 2019; Pyrenees, France: Mazier et al., 2006; Brittany: Marguerie, 1992).

3.4. sedaDNA analyses on core PADMé

3.4.1. Sampling strategy

In a sterile room with adequate tools and controlled conditions (IUEM, Plouzané, France), samples were taken in duplicate at intervals ranging from 10 to 20 cm along the PADMé core, excluding of the sandy

levels. This resulted in a total of 100 samples, plus control samples (tube kept open during sampling to control aerosol, one tube every 30 cm).

3.4.2. DNA extraction and library preparation

The ancient DNA (aDNA) extractions were performed at the P2GM platform (MNHM, Paris), using 200–250 mg of sediment per batch of 16, including one control extraction blank, and following the cold spin extraction protocol established by Murchie et al. (2021) from the initial protocol of Dabney et al. (2013). We performed library preparation according to a protocol slightly modified from Meyer and Kircher (2010), implementing the double indexing strategy proposed by Kircher et al. (2012) (lab work protocols are detailed in Data in Brief, David et al., *submitted*). All libraries were sequenced on an Illumina NovaSeq 6000 SP lane sequencing system (100 cycles).

Duplicates of each sample (and blanks) were pooled to make a single file to facilitate subsequent analyses. Adapters were removed in three consecutive rounds using cutadapt (Martin, 2011), with maximum error rate set at 0.5 (-e 0.5 parameter), FastP (Chen et al., 2018) and mapping using Geneious (*version 2023.1.2*, https://www.geneious.com) to retrieve any residual adapter though manual biocuration. Reads were then paired using BBTools (sourceforge.net/projects/bbmap/) and filtered to keep only those with an average quality above Q20 (–average_qual 20 restriction), no homopolymer (–trim_poly_g and –trim_poly_x options), and cut on the 3' part (–cut_right –cut_right_mean_quality 20 options). The sequences that successfully passed through these filters were subsequently merged, with a minimum overlap of 5 and deduplicated (optical duplicates) using FastP. Once these steps were completed, we retained reads with a minimum length of 35 bp.

3.4.3. Taxa classification

These reads were classified, without *a priori*, throughout the entire taxonomy, using Kraken (Wood and Salzberg, 2014) and a custom database constructed using non-redundant nucleotide records from NCBI. Sequences assigned to plant and mammal clades were retrieved and subsequently subjected to BLAST analysis (Altschul et al., 1990) against the nr database (updated August 2022). Concurrently, the specific taxa identified by Kraken, and likely indicative of livestock presence, agricultural practices, or anthropogenic environmental alterations, were chosen as targets for mapping against reference sequences (BWA aln: Li and Durbin, 2009/-l 1024; -o 2; -n 0.01; details in Data in Brief, David et al., *submitted*) and mapped sequences were subsequently subjected to a BLAST analysis (nr database, Blastn, word size = 11). If the BLAST result corresponded to a single taxon and exhibited the highest scores in terms of query cover and e-value, the name of that taxon was assigned to the sequence. If multiple taxa displayed identical scores, taxonomic rank was elevated incrementally, from genus to family and beyond, as necessary, until a conclusive assignation was achieved. These analyses were carried out by biocurators using in-house scripts and pipelines. Taxa identified in the controls (extraction blanks corresponding to samples without DNA) were excluded from the study and categorized as experimental "contaminants" (e.g., *Sus* sp., *Triticum* sp.), regardless of their number of sequences. The lists of reads recovered by the two approaches were compared in order to remove redundant information. Finally, the aDNA determination pattern and fragment length distribution were examined using mapDamage2 (Jónsson et al., 2013) for taxa with a sufficient number of merged reads, after alignment against each reference genome (see Data in Brief, David et al., *submitted*).

It is important to reiterate that the accuracy of taxonomic assignment relies heavily on the comprehensiveness of the reference database(s). Therefore, certain taxa may remain unidentified, or only identified to a high taxonomic rank (family, order …), if they are absent or inadequately represented in the database (Del Campo et al., 2014; Warinner et al., 2017; Velsko et al., 2018; Orlando et al., 2021). Furthermore, at this stage of the ongoing study, quantitative interpretation of the results remains difficult due to biases stemming from factors such as database completeness, post-mortem DNA damage and the suitability of analysis parameters and algorithms (for a comprehensive review, please refer to *Orlando* et al., *2021*).

3.4.4. Interpretation of sedaDNA data

For Viridiplantae, samples were considered if the number of reads assigned represented more than 0.1% of the total number of reads (other cases are shaded in grey in Figs. 6–8). Then, a cluster analysis was performed on these reads using the Past program v4.03 (Hammer et al., 2001; using the Bray-Curtis dissimilarity measure) to identify the main assemblages (Fig. 7) then used to underline the main fluctuations along the PADMé core and establish sedaDNA zonations (named S in Fig. 8). Following the recommendation of Pedersen et al. (2016), for each sample, reads were "normalized" to the total number of Viridiplantae sequences to obtain relative abundances and to smooth our taphonomic, taxonomic, or non-equivalent habitat biases. For mammalian taxa, due to their lower and more fluctuating sequence counts compared with plants, the inclusion criteria mandated a minimum of 5 reads if the taxon was detected in a single sample, or 3 reads if it was detected in multiple samples, and is reported as presence/absence data (Pedersen et al., 2016) in Fig. 10.

4. Results

4.1. Chrono-stratigraphical model and sedimentological description

4.1.1. Core ANE-C3

From the 18 AMS-^{14}C dates, a robust chronostratigraphic model was built, highlighting significant changes in sedimentation rates along the core (Fig. 2a). These varied from the highest values of ~7.5 mm/yr at the base of the core between 1094 and 974 cm (7.3–7.2 cal ka BP) to significantly lower values of ~1.6 mm/yr between 974 and 527 cm (7.2–4.5 cal ka BP), and ~2.2 mm/yr at the top of the sequence between 458 and 86 cm (3.2–1.6 cal ka BP). It is worth noting that the lowest sedimentation rates (0.55 mm/yr) are recorded between 527 and 458 cm, in an interval characterized by a reversed date, corresponding to a 1.3 kyr-long interval, and which may reflect a period of remobilization or very low sediment deposition (dark box in Fig. 2a).

Canonical Correspondence Analysis performed on XRF data showed a distinction between lithogenic elements Zr-Al-Si-K-Ti-Rb (correlated: r = 0.48–0.95), Ca-Sr elements (highly correlated: r = 0.97), covarying with carbonate content, and Mn, covarying with total organic content (Fig. 2c). To normalize XRF data, ratios based on anti-correlated elements were used: log(Ca/Ti) (biogenic carbonate versus terrigenous input; Croudace and Rothwell, 2015), log(Mn/Al) (organic content versus detrital signal).

The sedimentological (i.e., D50 and grain size distribution, as well as TOC and $CaCO_3$ percentages) and XRF analyses performed on this 12-m core (Fig. 2b) highlight differences in mineralogical and geochemical composition. The base of the core is made of weathered bedrock (from 1200 to 1130 cm). Thereafter, up to 780 cm, the sediments consist of silty clay to very fine sand interrupted, between 980 and 860 cm, by a peaty deposit indicated by a slight increase in TOC values (peak at 40%; yellow band in Fig. 2b). Also, two intervals (1050–970 cm and 835–778 cm; blue bands in Fig. 2b) show increases in D50 values (greater than 34 μm) associated with increases in $CaCO_3$ percentages (higher than the average value of 3%) and Ca/Ti-XRF values. Between 780 cm (6 cal ka BP) and 365 cm (2.9 cal ka BP), mean TOC values is 25%, with peaks reaching 70% reflecting dominant peaty deposits synchronous to increases in Mn/Al-XRF value (yellow bands in Fig. 2b). This trend is interrupted between 527 and 458 cm (4.5–3.2 cal ka BP) by a silty-clayey deposit with low TOC values. This interval, marked at its base by a slight increase in D50 values corresponds to the lowest sedimentation rates of the sequence (Fig. 2a and b). After 365 cm (2.9 cal ka BP), TOC values are lower than the mean value of 17% and Ca/Ti-XRF ratio values decrease (Fig. 2b). A short interval characterized by the increase in D50 values (peak of 80 μm) is seen between 250 and 215 cm. Finally,

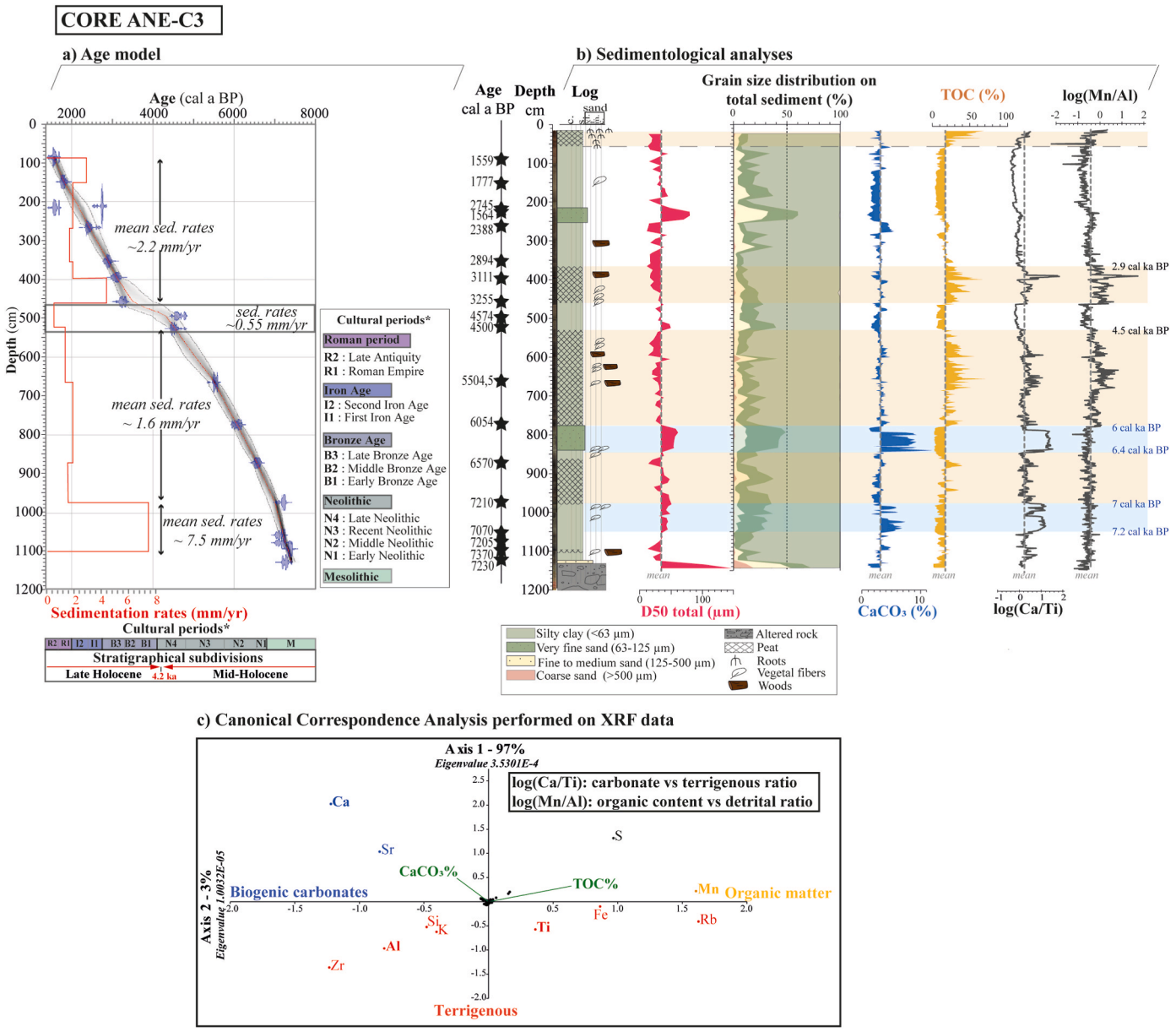

Fig. 2. Chronology and sedimentology of core ANE-C3. a) Age model established using the rbacon package (*Blaauw and Christen, 2011*) in R version 4.1.2 and expressed along cultural subdivisions for western Brittany (*Gorczyńska* et al., *2023a*) and stratigraphical intervals (*Walker* et al., *2019*). b) Sedimentological data plotted against depth (cm) with: total D50 (median), distribution among granulometric classes, carbonate ($CaCO_3$%) and Total Organic Carbon (TOC%) content, and X-ray Fluorescence (XRF) analyses. c) Canonical Correspondence Analysis applied to XRF data with projected variables including $CaCO_3$% and TOC%. Yellow bands: peaty deposits highlighted by increases in TOC values and Mn/Al-XRF ratio. Blue bands: synchronous excursions of D50, $CaCO_3$% as well as Ca/Ti-XRF ratio.

from 55 cm upwards, the top of the core is characterized by an increase in TOC values associated with the occurrence of modern roots.

4.1.2. Core PADMé

Among the 8 AMS-^{14}C dates carried out on the PADMé core (Table 2), 7 were used to build the chronostratigraphic model (Fig. 3a). The sedimentation rates appear steady, averaging 1.6 mm/yr along the core (Fig. 3a).

Grain size analyses performed on this 10-m core reveal that fine deposits (mean D50 of 33 µm) dominate the sedimentation. The base of the core is made of silty clay from 1000–960 cm, followed by peaty deposits between 960 and 580 cm (Fig. 3b). Thereafter and up to the top of the core, the sedimentation consists of silty-clayey deposits interrupted between 310–300, 240–200 and at 105 cm by medium to coarse sandy deposits. From 50 cm onwards, peaty deposits are found, associated with modern roots.

4.2. Palynological results on the ANE-C3 core

4.2.1. General description of the palynofacies

The palynological study of the ANE-C3 core focused on pollen assemblages and Non-Pollen Palynomorphs (NPPs), mainly represented by spores, and two marine bio-indicators: dinocysts and foraminiferal linings (Fig. 4a). The lower part of the core, from the base to 780 cm, is marked by the presence of inner to outer neritic dinocyst taxa (main identified taxa: *Spiniferites bentorii, Spiniferites ramosus, Operculodinium centrocarpum, Spiniferites membranaceus*) and foraminiferal linings (blue bars in Fig. 4a), which both increase simultaneously with $CaCO_3$ values (blue bands in Fig. 2b), and more particularly during the 835–778 cm interval (dinocysts and foraminifera represent 4% and 9% of the counted

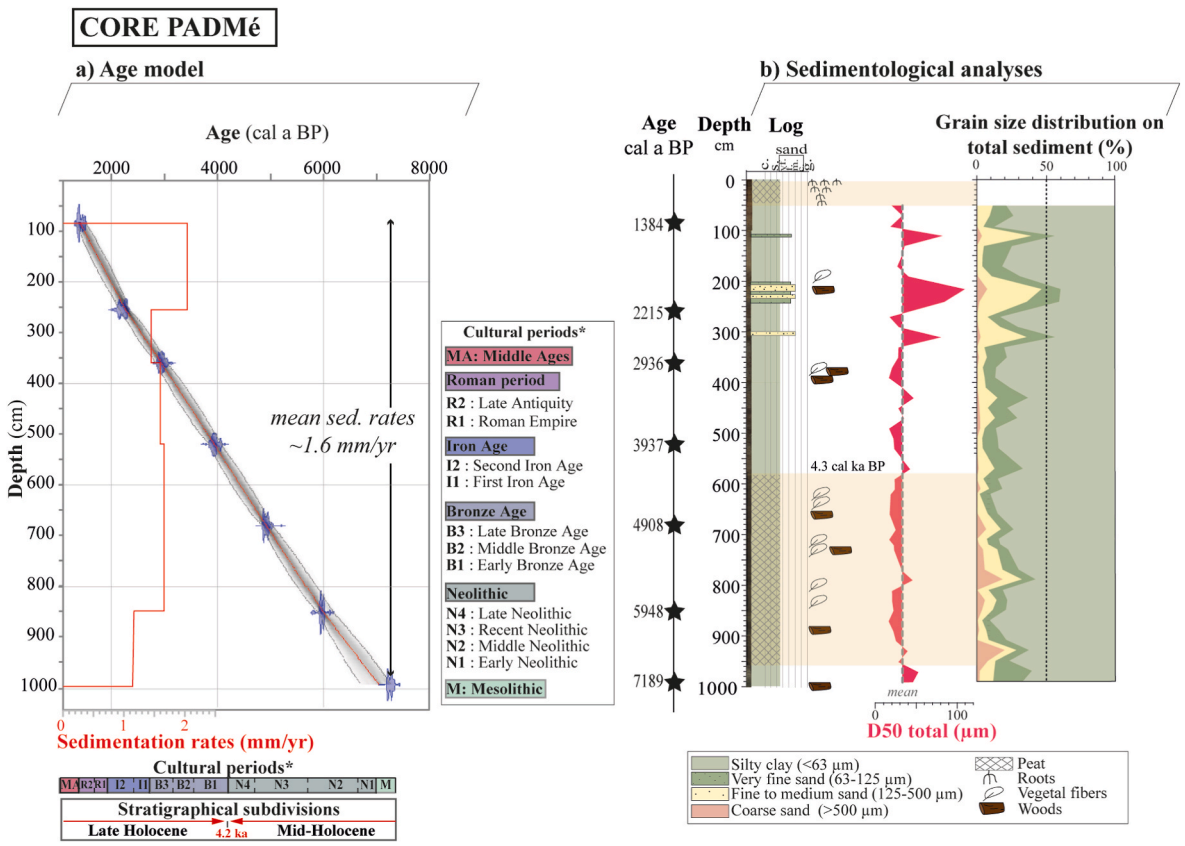

Fig. 3. Chronology and sedimentology of core PADMé. a) Age model established using the rbacon package (*Blaauw and Christen, 2011*) in R version 4.1.2 and expressed along cultural subdivisions for western Brittany (*Gorczyńska* et al., *2023a*) and stratigraphical intervals (*Walker* et al., *2019*). b) Grain size analyses plotted vs. depth (cm) with total D50 (median) and distribution among granulometric classes. Yellow bands: peaty deposits.

palynomorphs, respectively; Fig. 4a). Subsequently, the occurrences of marine bio-indicators decrease until they disappear after 655 cm (5.4 cal ka BP).

4.2.2. Pollinic signal description

The CONISS clustering of pollen assemblages led to the establishment of 4 main palynozones (P1 to P4; Fig. 4) highlighting the main vegetation changes. In addition, the cluster analysis performed on pollen percentages allows the composition of 6 main pollen assemblages, as shown in Fig. 5. Colors were assigned to each cluster of the assemblages which were then located along the ANE-C3 core, allowing the pollen zonations to be confirmed (Fig. 4c).

Along the ANE-C3 core, a total of 108 different pollen taxa were recognized, with an average of 33 pollen taxa per level counted (Fig. 4b). Mean species richness reaches 31 and 30 taxa in zones P1 and P2, respectively, before increasing to 35 and 38 taxa within zones P3 and P4, respectively (see diversity and related Margalef diversity index in Fig. 4b).

More precisely, zone P1 is characterized by high percentages of arboreal taxa (~72%; Fig. 4c). *Corylus* (~42%) and *Quercus* (~23%) are the dominant taxa, alongside Amaranthaceae (~5.5%) and *Betula* (~2%), both reaching their highest percentages of the whole sequence.

Zone P2 is marked by the increase in *Corylus* (~61%) and decrease of *Quercus* (~14%), *Pinus* (from ~2% in zone P1 to ~0.6% in P2) and *Betula* (~0.5%). The Amaranthaceae, whose percentages reach ~5% in subzone P2a (similar to values recorded in P1), decline to under 1% in subzone P2b. Arboreal taxa reach their highest percentages in subzone P2c (88%) mainly driven by *Corylus* percentages (~71%; Fig. 4c). In parallel, *Quercus* (peak of 22%), *Hedera* (peak of 10%), *Ulmus-Tilia* (peak of 4%) and then *Ilex* (peak of 2%) successively increase. From the subzone P2d, *Corylus* percentages decrease (~64%), while ruderal and arable weed taxa progressively increase (~1%).

A drastic change in the pollen assemblages occurs in zone P3, marked by the decline of arboreal taxa percentages (from 74% to a minimum of 55%) and simultaneous rise of herbaceous ones (from 25% to a maximum of 44%, Fig. 4c). During this interval, Poaceae represent a large part of the herbaceous taxa. Furthermore, ruderal and arable weed taxa gradually increase (~1.5%; red curve in Fig. 4c), as well as occurrences of *Cerealia*-type.

Finally, zone P4 is marked by a new threshold characterized by an increase in arable weed and ruderal taxa (~3.5%), accompanied by *Plantago lanceolata*, Asteroideae, and Cichorioideae (orange curves in Fig. 4c). Arboreal taxa continue to decline sharply in subzone P4a, while occurrences of *Cerealia*-type pollen reach their maximum (Fig. 4c). Within subzone P4b, *Corylus* percentages increase while those of Poaceae decrease (~33%–~45%). However, ruderal and arable weed taxa, as well as Asteroideae, Cichorioideae, and *Plantago lanceolata*, continue to increase (Fig. 4c). The last subzone, P4c, is characterized by the drastic decline in arboreal taxa (to a minimum of 15%) and the marked increase in herbaceous taxa (Poaceae reach ~41%).

4.3. SedaDNA results on the PADMé core

4.3.1. General description of sedaDNA results

Along the core, an average of 791,200 reads (>35bp) per sample was obtained after the first pre-processing steps (min: 293,550/max: 1,849,770), including 7 samples with more than 1,000,000 reads (at 170, 590, 610, 660, 680, 850, 870 cm). An average of less than 1% reads without duplicates was assigned (min: 0.7%/max: 1.4%; Fig. 6a). Such low values are expected and are in the range of previous aDNA studies (Carpenter et al., 2013; Pedersen et al., 2016; Murchie et al., 2021; Green et al., 2010).

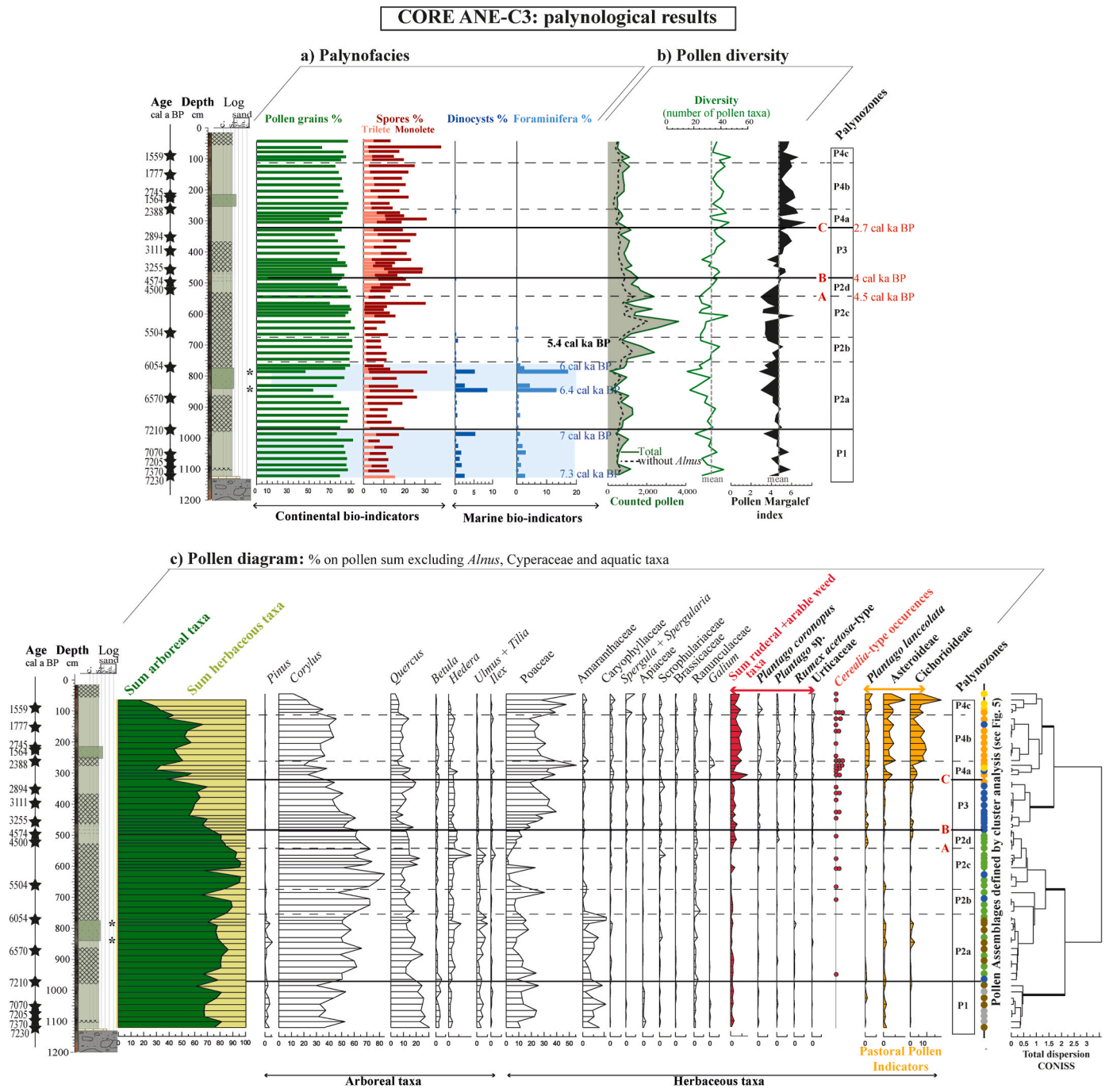

Fig. 4. Palynological results plotted vs. depth (cm), along the log of the ANE-C3 core (see Fig. 2 for the legend of the log). a) Palynofacies composition including counted palynomorphs. b) Pollen diversity indexes (i.e., number of pollen grains counted, number of pollen taxa, and Margalef diversity index. d) Major taxa percentages (>1.5%) of the pollen assemblage calculated on the total pollen sum excluding some local taxa (i.e., Cyperaceae, aquatic taxa and riparian trees, mainly represented by *Alnus*). Palynozones: defined by a CONISS clustering (this figure) and a cluster analysis (see Fig. 5). Blue bands: synchronous excursions of marine bio-indicators percentages, CaCO3% and Ca/Ti-XRF ratio (see Fig. 2). Limits A to C indicate the main anthropic thresholds. Asterisk: level 845 and 785 cm with less than 215 and 140 counted pollens grains, respectively.

To highlight the main changes in the plant community, a cluster analysis was performed on the sedaDNA Viridiplantae dataset, leading to the identification of two main groups (A-B) and 3 subgroups (SA1-SA3) (Fig. 7), which ultimately led to the definition of 9 sedaDNA zones along the PADMé core (S1-S9; Fig. 8). Group A comprises samples in which an average of 50% of assigned reads are attributed to bacteria (min: 35%/max: 69%). Conversely, a mean of 29% of reads are assigned to Viridiplantae (mean: 20%/min: 9%/max: 36%) and a mean of 9% Metazoa (ranging from 5% to 17%; Fig. 6a). These samples also have more than 0.1% of the total number of reads assigned to Viridiplantae (Fig. 7a). In contrast, group B gathers samples in which an average of 68% of assigned reads are attributed to bacteria (min: 46%/max: 84%) and only 6% to Viridiplantae (min: 2%/max: 9%) and 6.6% to Metazoa (min: 2%/max: 11%) (grey bands in Fig. 6a). These samples have less than 0.1% of total reads assigned to Viridiplantae (Fig. 7a). Considering the limited number of assigned sequences in the samples from group B, it is important to interpret these results with caution. For group A, which show a notably higher assignment level, especially at depths of 310, 610,

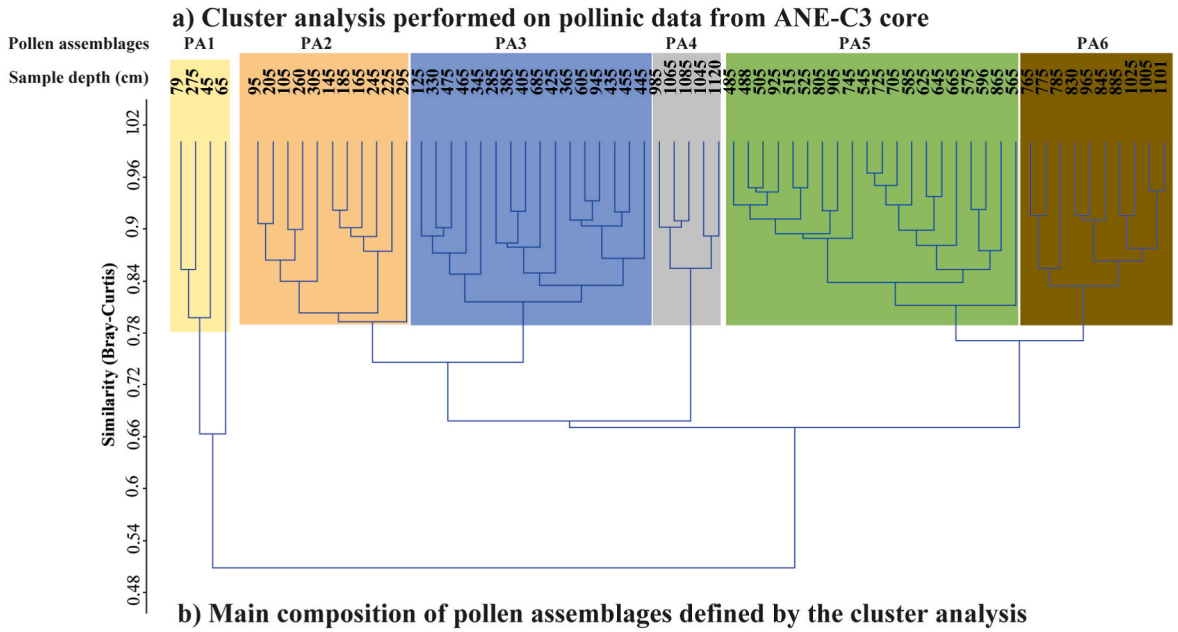

b) Main composition of pollen assemblages defined by the cluster analysis

Assemblages	Main taxa (>2%)	Environmental interpretation
PA1	**Poaceae 47%** / *Corylus* 20% / **Cichorioideae** *8%* / *Quercus* 6% / **Asteroideae 4% / Ruderal and arable weed taxa 3%** / ***Plantago lanceolata* 2%**	Open and anthropized environment (agro-pastoral practices)
PA2	*Corylus 34%* / **Poaceae 31%** / *Quercus* 8% / **Cichorioideae 7% / Asteroideae 3% / Ruderal and arable weed taxa 4%**	Open and anthropized environment (agro-pastoral practices)
PA3	***Corylus 49%*** / **Poaceae 26%** / *Quercus* 11% / *Hedera* 2%	Landscape opening
PA4	***Corylus 33%*** / ***Quercus* 26%** / Poaceae 19% / **Amaranthaceae 7%** / *Betula* 2% / *Ulmus+Tilia* 2%	Proximity of maritime marsh + Wooded environment
PA5	***Corylus 67%*** / ***Quercus* 14%** / Poaceae 7% / *Hedera 3%*	Wooded environment
PA6	***Corylus 50%*** / ***Quercus* 19%** / Poaceae 11% / **Amaranthaceae 5%** / *Ulmus+Tilia* 3% /*Hedera* 2% / *Pinus* 2%	Proximity of maritime marsh + Wooded environment

Fig. 5. Results of the cluster analysis performed on pollinic data from core ANE-C3 (Bray-Curtis dissimilarity index): a) clustering of the samples showing a similar composition and b) main pollen composition of the assemblages defined by the cluster analysis.

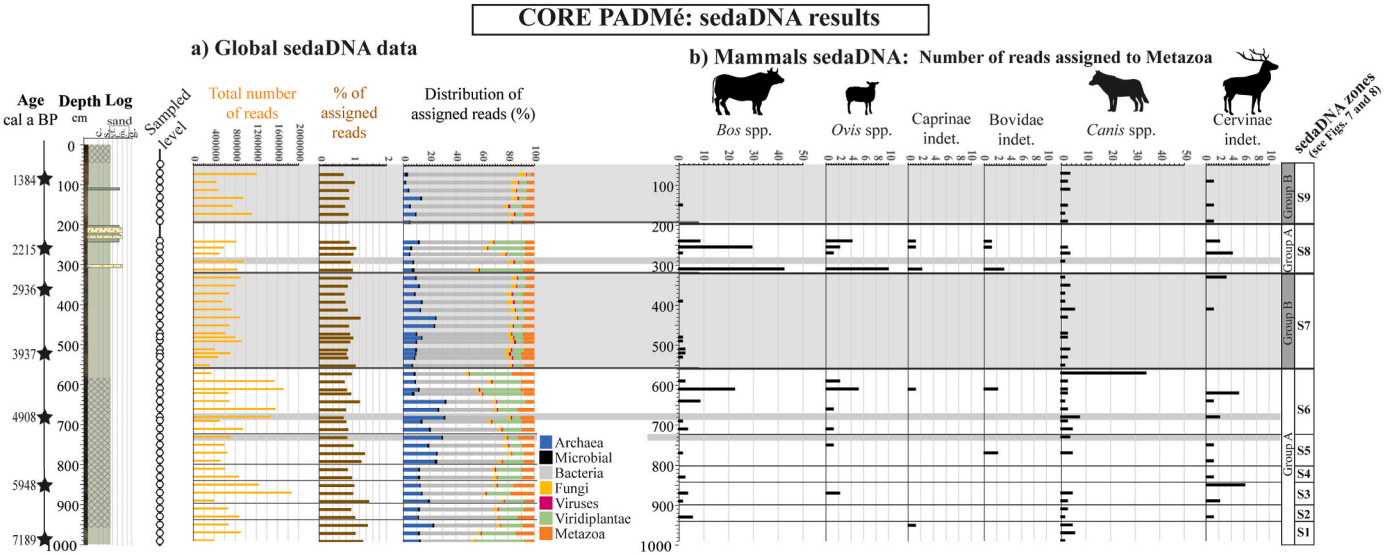

Fig. 6. First part of the sedaDNA results plotted vs. depth (cm) along the log of core PADMé (see Fig. 3 for the legend of the log). a) Global sedaDNA data (total number of reads detected, percentages of assigned reads and their main distribution groups). b) Number of reads assigned to selected Metazoa. Grey bands: intervals with less than 0.1% of total reads assigned to Viridiplantae per level. sedaDNA zone defined by a cluster analysis performed on Viridiplanteae assigned reads (see Figs. 7 and 8).

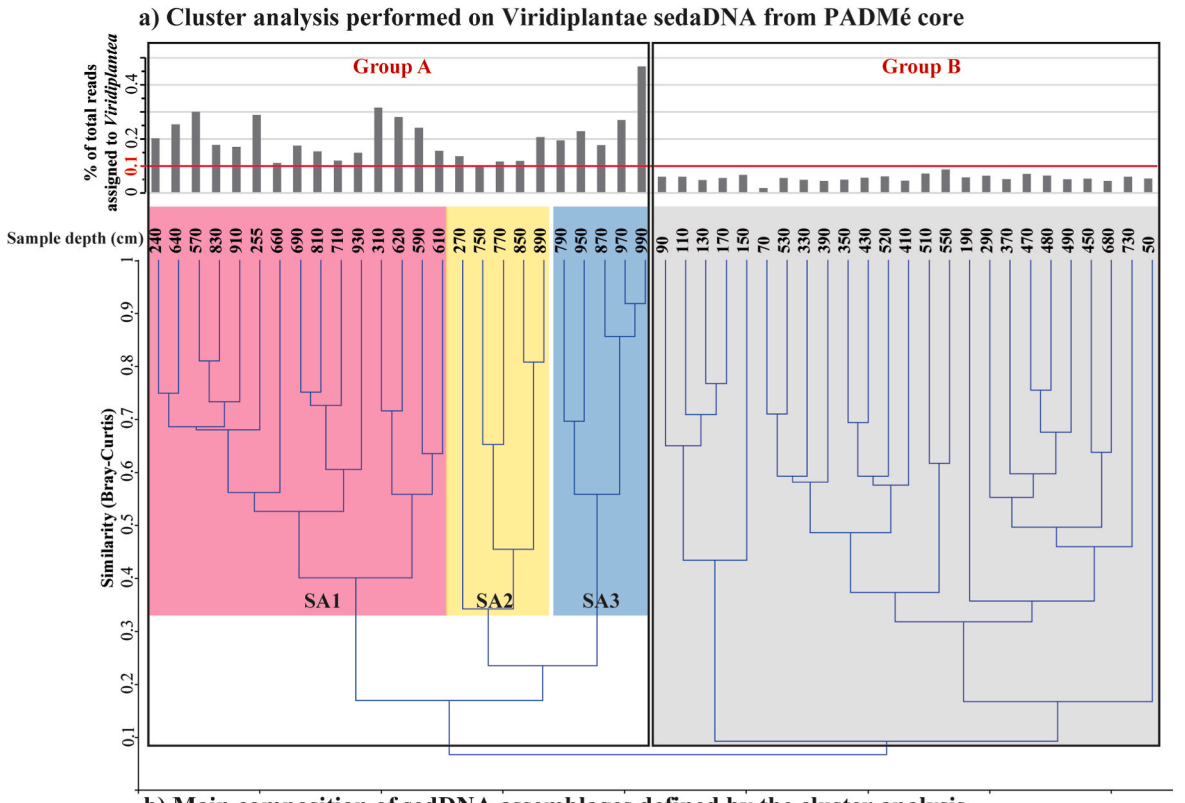

b) Main composition of sedDNA assemblages defined by the cluster analysis

SedaDNA asemblages	Mean number of assignated reads to plant node (only taxa > 10 assignated reads)										
SA1	Betulaceae	*Corylus*	*Alnus*	Poaceae	*Carpinus*	*Quercus*	Ranunculaceae	*Callitriche*	*Betula*	Fagaceae	Rosaceae
	641	618	466	197	161	152	80	72	57	31	45
	Prunus	*Malus*	Cyperaceae	Fabaceae	*Juncus*	Asteraceae	Juglandaceae	*Rubus*			
	34	29	21	17	15	11	11	11			
SA3	Poaceae	Cyperaceae	*Phragmites*	*Callitriche*	*Corylus*	Betulaceae	*Quercus*	*Alnus*			
	494	348	118	93	83	44	19	19			
SA3	Poaceae	*Phragmites*	*Corylus*	Cyperaceae	Betulaceae	*Juncus*	*Callitriche*	*Quercus*	Asteraceae	*Alnus*	*Carpinus*
	4053	1300	175	163	113	98	58	38	32	26	17

Fig. 7. Results of the cluster analysis performed on Viridiplantae sedaDNA data from the PADMé core (Bray-Curtis dissimilarity index): a) clustering of the samples showing a similar composition and b) main assigned reads composition of the assemblages defined by the cluster analysis.

620, and 640 cm, the cluster analysis highlights 3 subassemblages (SA1 to SA3) described in Fig. 7b. Colors were assigned to each of the A subgroups and replicated along the PADMé core (Fig. 8). The strong disparity between the two groups A and B suggests that variability in sediment mineralogical composition along the core could profoundly affect DNA mineral associations and patterns of DNA preservation and retention. For these reasons, our approach to interpreting sedaDNA results focused on assessing the fluctuations in relative taxa abundances through time. Throughout the core, the distribution of assigned reads to microbes, fungi, and viruses showed a relatively consistent pattern. In this study, our analysis was centered on Viridiplantae and on mammals for the Metazoa clade.

4.3.2. *Metazoa dataset description*

For this part of the study, we chose to describe mammal sedaDNA data based on the sedaDNA zonation established using the Viridiplantae data (S1–S9; Fig. 6b). Among mammals, the most commonly identified reads are Bovidae, among which *Bos* spp., *Ovis* spp. and undetermined Caprinae. *Ovis* spp. are detected in S3, S5, S6, S8, exceeding 5 assigned reads in samples 610 (S6) and 310 cm (S8). *Bos* spp., found in all zones, reach the highest values in S6 (22 assigned reads at 610 cm) and S8 (42 and 29 assigned reads in samples 310 and 255 cm respectively). Indeterminate Caprinae and Bovidae are scarce and do not exceed 2 and 3 assigned reads. *Canis* spp. are the most continuously recorded taxa all along the core, even in poorly assigned samples, with the highest values being reached at 590 cm (34 assigned reads; S6). Cervinae are frequently recorded and exceed 5 assigned reads in samples 850 (S3) and 620 cm (S6; Fig. 6b).

Canis spp. are continuously recorded all along the core, including in the samples of group B (poorly assigned apart from Bacteria), raising questions about these results. Other studies have noticed the frequent presence of *Canis* spp. in DNA as traces (Giguet-Covex et al., 2019) but it is not expected to detect this genus in samples where almost no plants or mammals are identified significantly in the studied succession. However, no *Canis* reads were identified in any of the controls. We also noticed that among the *Canis* reads along the core, 75 reads remain undetermined at the species level, whereas 30 and 21 reads could be attributed to the wolf (*Canis lupus*) and the dog (*Canis lupus familiaris*), respectively. Wolf presence remains scarce in archaeozoological data and its even rare in sedimentary records, whereas the dog is more easily reported because of its domestic status and proximity to humans. The high amount of wolf DNA identified in the results could either be explained by sequencing errors or artefactual substitutions inherent to aDNA that could have resulted in modification of the DNA sequence and consequently to assignment errors, particularly for such close genomes. We also hypothesize that the number of reads attributed to the wolf and

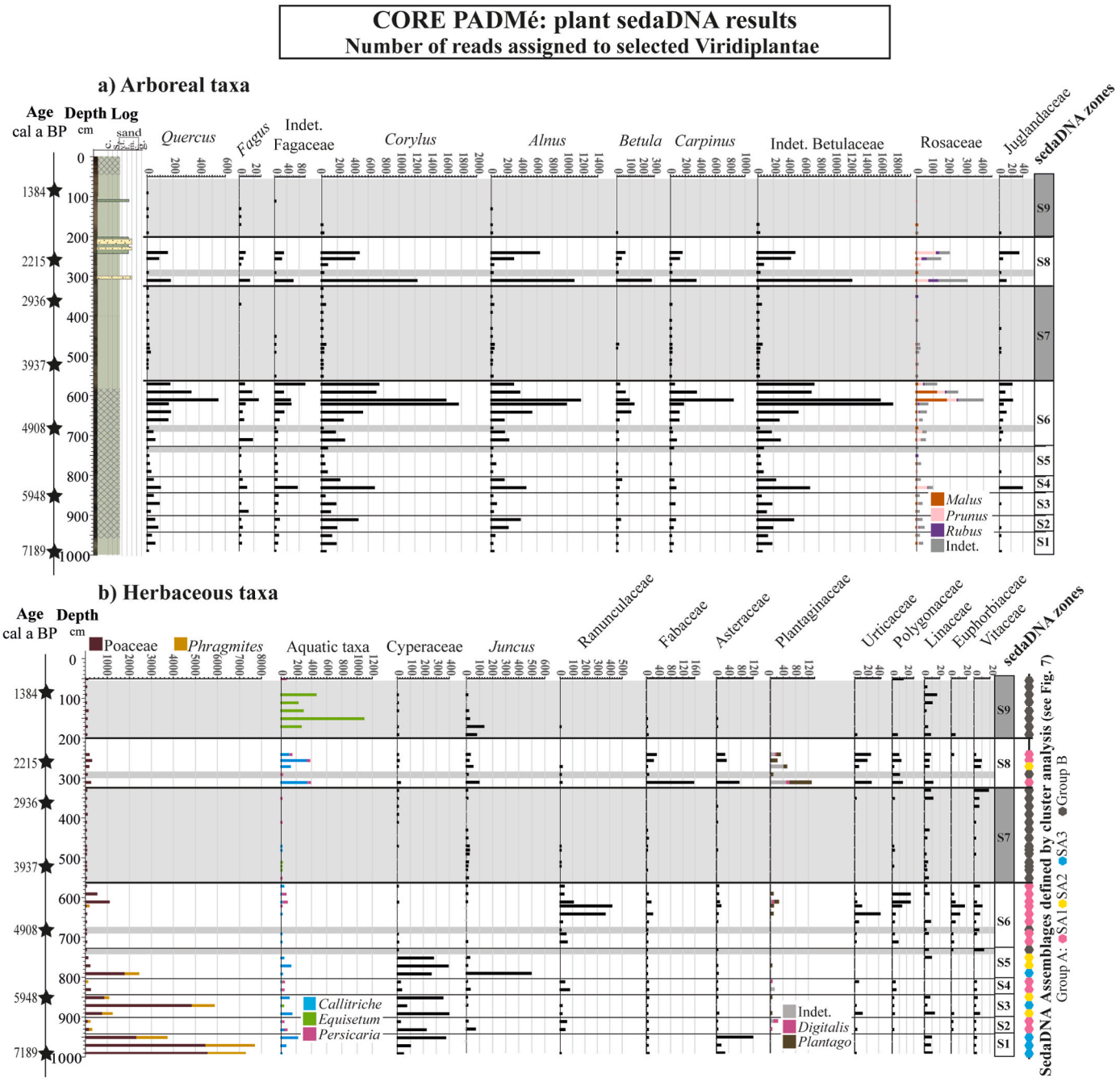

Fig. 8. Second part of the sedaDNA results plotted vs. depth (cm), along the log of core PADMé (see Fig. 3 for the legend of the log). Number of reads assigned to selected Viridiplantae, a) arboreal taxa and b) herbaceous taxa. Grey bands: intervals with less than 0.1% of total reads assigned to Viridiplantae per level. sedaDNA zone defined by a cluster analysis performed on Viridiplantae assigned reads (see Fig. 7).

its presence throughout the core could have been caused by contamination between layers (which could result from the decomposition of a wolf carcass in a higher level) or by exogenous contaminations, although no evidence of post-depositional reworking was observed.

4.3.3. *Viridiplantae sedaDNA dataset description*

The fluctuations in vegetation observed through the sedDNA datasets were delineated using cluster analysis, revealing 9 distinct zones across the PADMé core (S1 to S9, Fig. 8). The first 5 sedaDNA zones located in the peaty base of the core (S1 to S5) are characterized by a notable abundance of reads, predominantly assigned to the Poaceae and Cyperaceae families. These families account for the most discernible DNA content within these levels, whereas their abundance diminished in the subsequent sections of the sequence (above 730 cm). Within this S1-S5 interval, the results reveal alternating vegetation assemblages.

Zones S1 (3 samples from 990 to 950 cm) and S3 (3 samples from 890 to 850 cm) are characterized by high proportions of Poaceae reads (mean of 4500 reads in S1 and of 2212 reads in S3), mostly assigned to *Phragmites* (~1680 reads in S1 and 463 reads in S2; Fig. 8b). Signals from *Callitriche* (an aquatic Plantaginaceae) and Asteraceae are also noteworthy within these assemblages. The arboreal taxa reads are mainly assigned to *Corylus* (~200 reads in S1 and S3) and indeterminate Betulaceae (~100 reads; Fig. 8a).

Zones S2 (2 samples at 930 and 910 cm) and S4 (2 samples at 830 and 810 cm) are characterized by a decline in the previously mentioned herbaceous taxa. Arboreal reads are dominant, primarily composed of

Betulaceae (mean of 793 reads in S2 and 1037 reads in S4), among which *Alnus* (~290 reads in S2 and 299 in S4) and *Corylus* (~130 reads in S2 and 225 in S4) appear to be the predominant genera, alongside other taxa of the same family (*Betula, Carpinus* and indeterminate Betulaceae; Fig. 8a). To a lesser extent, the Fagaceae family is also represented, with *Quercus* (~63 reads in S2 and 68 in S4), *Fagus,* and indeterminate Fagaceae.

In zone S5 (4 samples from 790 to 730 cm), the assemblage bears similarities to both S1 and S3, characterized by the consistent presence of Cyperaceae (230 reads on average) and *Callitriche* occurrences, albeit with a reduced Poaceae signal. At 790 cm, *Juncus* reads (approximately ~490) reach their highest occurrences along the core, coinciding with a substantial proportion of Poaceae (1800 assigned reads including 535 assigned to *Phragmites*; Fig. 8b).

Zone S6 (9 samples from 710 to 570 cm dominated by peaty deposits) is distinguished by the rise of all arboreal taxa, mainly dominated by Betulaceae and Fagaceae. Notably, Betulaceae are primarily represented by *Corylus* (800 reads on average), *Alnus* (~430 reads), and *Carpinus* (~185 reads) alongside less frequent *Betula* and abundant indeterminate Betulaceae reads. The Fagaceae are represented by *Quercus* (~180 reads), some *Fagus* (peak at 25 reads) and indetermined reads. Some Rosaceae (~110 reads) are also identified, among which *Malus* and *Prunus,* together with traces of Juglandaceae (peak at 20 reads), for which reads were assigned to *Juglans*, already present in S4 (Fig. 8a). Among herbaceous taxa, the S6 is characterized by its abundant Ranunculaceae content (reaching a maximum in samples 640 and 620 cm) accompanied by an assemblage including Urticaceae, Polygonaceae, Euphorbiaceae, and Vitaceae while Fabaceae, Asteraceae and Plantaginaceae are present only in trace amounts, similar to aquatic taxa (Fig. 8b).

Zone S7 (14 samples from 550 to 350 cm dominated by silty deposits) corresponds to group B (grey band in Fig. 8) and presents less than 0.1% of total reads assigned to Viridiplantae, thus preventing characterization of the vegetation dynamics.

Zone S8 (5 samples from 310 to 240 cm taken in silty to very fine sand deposits) is marked by the resurgence of the arboreal signal primarily dominated by Betulaceae, notably *Corylus, Alnus*, and undetermined taxa. *Betula* and *Carpinus* are also present to a lesser extent. Additionally, Fagaceae (notably *Quercus*) and Rosaceae co-occur with Juglandaceae in smaller proportions (Fig. 8a). In this zone, among herbaceous taxa, we observe a resurgence of *Callitriche* and *Juncus*, and an increase of reads assigned to Fabaceae, Asteraceae, and Plantaginaceae (Fig. 8b).

Finally, in zone S9 (8 samples from 190 to 50 cm, dominated by silty deposits), despite the low number of reads assigned to plants (group B), *Equisetum* was detected and was most likely the dominant taxon, reaching 460 reads on average between 170 and 90 cm.

4.4. Comparison of palynological and sedaDNA records

This study provides a preliminary analysis of the DNA dataset, which involved an initial comprehensive assignment step using Kraken2 without any prior assumptions. Our research, then narrowed down to focus on specific genomes among the Viridiplanteae and mammal taxa. Through our approach, we generally identified less taxa from the sedaDNA record (~67 taxa) than by pollinic analysis (~108 taxa).

Among trees and shrubs, the Plouescat palynological record identified 26 taxa, with 8 accounting for a substantial proportion (mean occurrences >2%), while 17 taxa were identified in the sedDNA record. The dominant taxa (*Alnus, Corylus, Quercus* and *Betula)* were recorded by both proxies, as were *Carpinus*, *Castanea, Fagus*. Other arboreal taxa detected in the pollinic analysis (i.e., *Pinus, Hedera*, *Ilex*, *Ulmus/Tilia*) were not recorded by sedaDNA, probably due to their absence from the site and their long-distance transport origin. Juglandaceae (i.e., *Juglans*) were only detected by sedaDNA analysis, implying the absence of walnut trees from the site. The detection of walnut DNA traces could have resulted from nuts or wood remnants imported to the site. Rosaceae, which were identified only at the family taxonomic rank in palynological analysis, are detected only as rare occurrences in our pollen dataset, while sedaDNA analysis identified the distinctive presence of *Malus, Prunus,* and *Rubus* (Fig. 9a).

Among herbaceous taxa, 82 taxa were identified in the pollinic record, of which 10 are significant (mean occurrences >2%), while 50 taxa were identified by sedaDNA analysis. Poaceae, Amaranthaceae, Asteroideae, Cichorioideae, Cyperaceae, Ranunculaceae, Urticaceae, and Fabaceae (only identified at the family level in the pollinic analysis) are present in both datasets. Plantaginaceae, Polygonaceae, and Euphorbiaceae were identified by both proxies, but with some different taxa. Juncaceae (i.e., *Juncus*) and *Equisetum* were only recorded in the sedaDNA record, which could be because, while these marsh plants can reproduce sexually (*Equisetum* through short lifespan microspores and *Juncus* through insect pollination), they primarily reproduce vegetatively through their rhizomes or tubers. In contrast, Caryophyllaceae (comprising *Spergularia/Spergula*), Apiaceae, Brassicaceae, and Scrophulariaceae are only found in the pollen record (Fig. 9a). Taxa with low occurrences in the pollinic data (0.1–2%, and thus not represented in pollen spectra) were not detected in sedaDNA data (e.g., Ericaceae, *Artemisia*, Crassulaceae, *Centaurea* sp., Saxifragaceae, *Trifolium*, Liliaceae, etc.), indicating that these taxa were scarce in the surrounding vegetation cover. Finally, aquatic taxa are represented by *Callitriche, Equisetum,* and *Persicaria* in the sedaDNA sequence, and mainly by scarce occurrences of *Myriophyllum, Typha/Sparganium*, *Alisma plantago aquatica, Lemna* and *Potamogeton* in the pollinic records (<0.6%).

The incomplete overlap between pollen and sedaDNA taxonomic records, which is summarized in Fig. 9a, is not surprising and aligns with expected outcomes that can be attributed to different processes (Fig. 9b). If a taxon can be identified via pollen records but not through sedaDNA analysis, this may be attributable to DNA preservation issues, absence from genomic databases, or DNA dominance effect hindering the detection of rare sequences. Furthermore, some plants, particularly trees (e.g., *Pinus, Ilex)*, produce abundant pollen grains that can be transported over long distances, potentially leading them to degrade and lose cellular content (and thus DNA), while remaining identifiable by palynological analysis. Conversely, taxa identified by DNA but not detected in pollen analysis correspond either to an inability to obtain fine taxonomic resolution through pollen characteristics, which can typically only identify to the family level (particularly for some taxa Poaceae or Rosaceae) while DNA discriminates genera/species, or to plants with low pollen production due to vegetative propagation (e.g., rhizomes), or unsuitable ecological conditions (seasonality, for example).

In the case of our study, all the tree taxa recorded in the pollinic but not in sedaDNA analysis are important producers (e.g., *Pinus*, *Hedera*, etc.). In addition, pollen grains of anemophilous and hydrophilous taxa can be transported over long distances and reflect local to regional landscapes, whereas sedaDNA data reflect more local sources and thus local variation in biodiversity (as previously mentioned by Capo et al., 2021; Parducci et al., 2013, 2019) through a better detection of low pollen producer and entomophilous species. However, allochthonous sources in sedaDNA should not be completely excluded. Eroded materials containing DNA can be brought in from the catchment area (Giguet-Covex et al., 2019) by runoff, as may have been the case in our coring site located close to the Kerallé river.

5. Environmental evolution and anthropogenic signal in the Kerallé valley since 7.3 cal ka BP

Retrieved within a radius of 10–15 m, the two cores ANE-C3 and PADMé, show different sedimentary successions, mainly explained by environmental variability in a context of alluvial channel migration. In the following discussion, all the data are expressed as calibrated radiocarbon ages (cal ka BP), which allow the direct comparison of ANE-C3 and PADMé datasets (Fig. 10).

a) Comparison of the main plant taxa occurrences detected by palynological, and sedaDNA analyses

TREES AND SCHRUBS			
Family	Family / Genera	Pollen	SedaDNA
Aquifoliaceae	*Ilex*	✓	
Araliaceae	*Hedera*	✓	
Betulaceae	*Alnus*	✓	✓
	Corylus	✓	✓
	Betula	✓	✓
	Carpinus	✓	✓
Fabaceae	*Cytisus, Genista*	✓	
Fagaceae	*Quercus*	✓	✓
	Fagus	✓	✓
	Castanea	✓	✓
Juglandaceae	*Juglans*		✓
Pinaceae	*Pinus*	✓	
Rosaceae	Pollen: Rosaceae sp.	✓	
	SedaDNA: Rosaceae sp.		✓
	Malus		✓
	Prunus		✓
	Rubus		✓
	Ulmus+Tilia	✓	

HERBS			
Family	Family / Genera	Pollen	SedaDNA
Amaranthaceae		✓	✓
Apiaceae		✓	
Asteraceae (Asteroideae)		✓	✓
Asteraceae (Cichorioideae)		✓	✓
Brassicaceae		✓	
Callitrichaceae	*Callitriche*		✓
Caryophyllaceae		✓	
Cyperaceae		✓	✓
Equisetaceae	*Equisetum*		✓
Euphorbiaceae	Pollen: *Mercurialis, Euphorbia* SedaDNA: *Euphorbia*	✓	✓
Fabaceae		✓	✓
Juncaceae			✓
Linaceae		✓	✓
Poaceae	Pollen: Poaceae sp., *Cerealia-type* SedaDNA: Poaceae sp., *Phragmites*	✓	✓
Plantaginaceae	Pollen: *P. lanceolata, P. coronopus, Plantago* sp. SedaDNA: *Plantago* sp., *Digitalis*	✓	✓
Polygonaceae	Pollen: *Rumex* sp., *Polygonum sp.* SedaDNA: *Rumex* sp., *Persicaria*	✓	✓
Ranunculaceae		✓	✓
Scrophulariaceae		✓	
Urticaceae		✓	✓
Vitaceae			✓
	Typha-Sparganium	✓	
	Myriophyllum	✓	

Absent	% of maximum occurrences
✓ Present	> 30%
	10-30%
	1-10%
	<1%

taxa only identified in pollen dataset
taxa only identified in sedaDNA dataset
taxa identified in sedaDNA and pollen dataset at a different taxonomic level

b) Conceptual scheme illustrating the probable origin of pollen grains and Viridiplantae DNA, and multiple biases

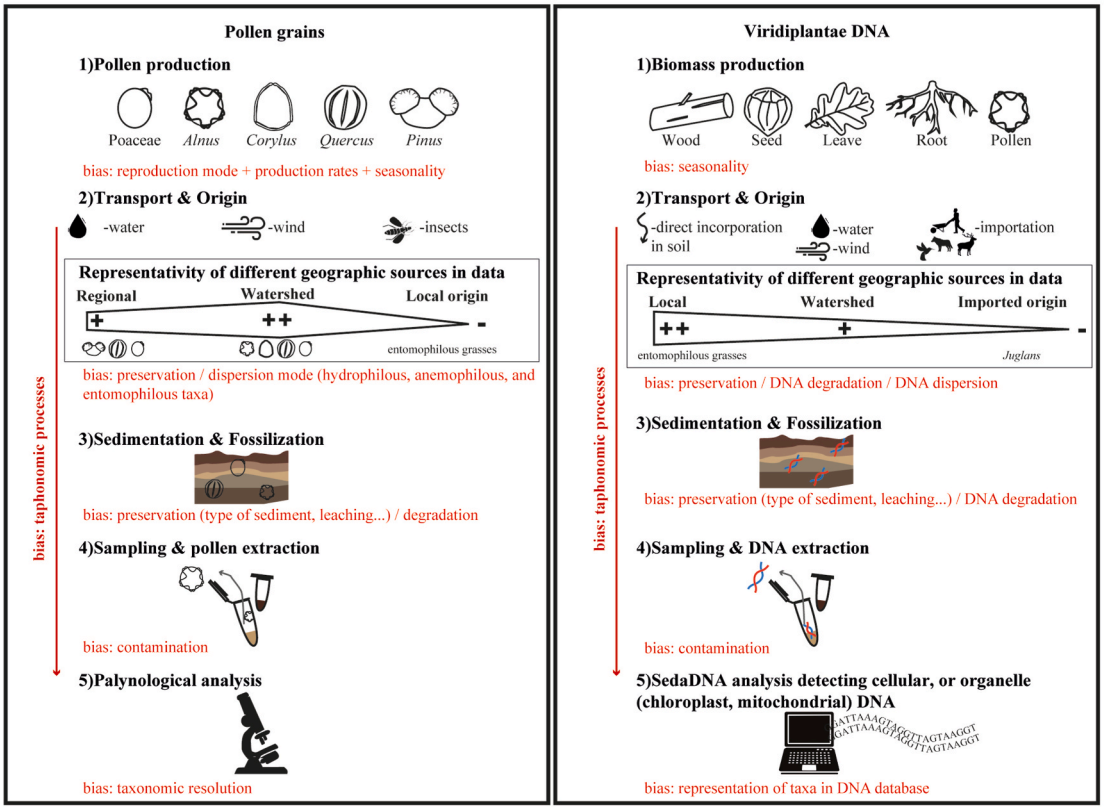

Fig. 9. Differences between pollinic and Viridiplantae sedaDNA datasets. a) List of the main plant taxa identified by palynological (core ANE-C3) and/or sedaDNA (core PADMé) analyses. Percentages indicating the maximum occurrences along the cores, calculated based on the total sum of counted pollen grains or relative abundance of Viridiplantae DNA. b) Schema of discussion of the origin of pollen and Viridiplantae DNA fossilized in sedimentological archives and biases for both.

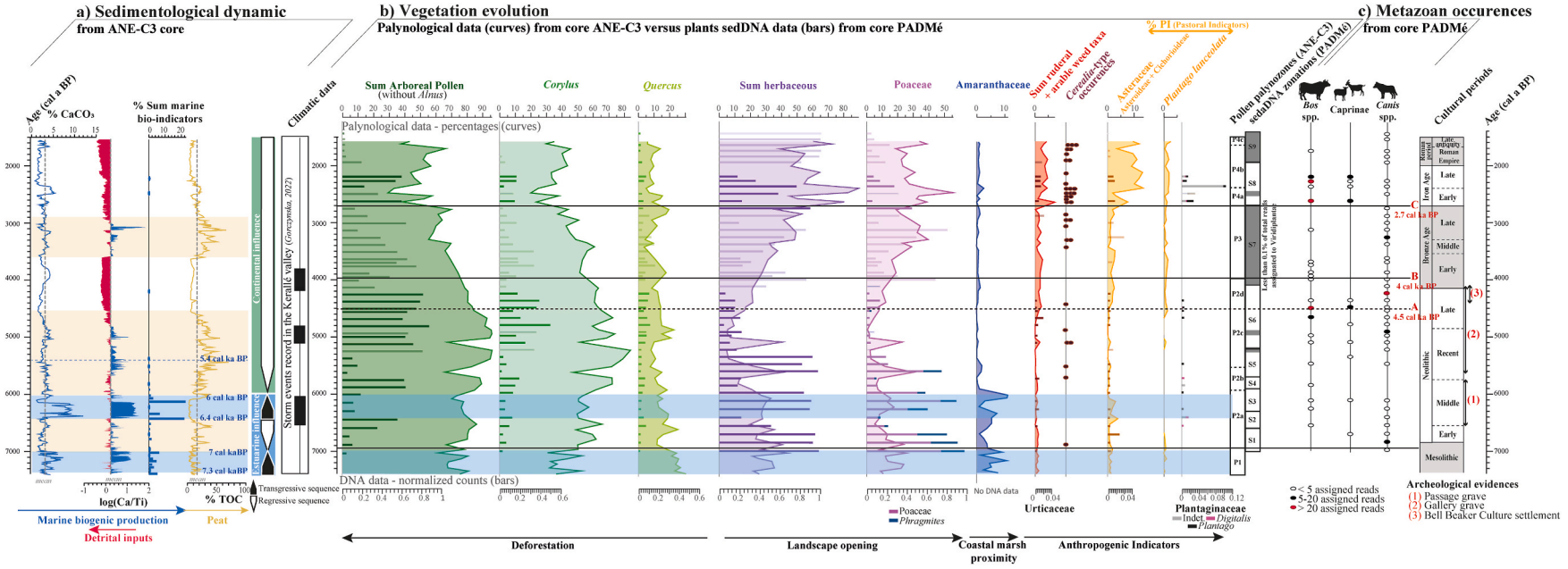

Fig. 10. Selected a) sedimentological data (core ANE-C3), b) palynological (core ANE-C3) and plant sedaDNA (core PADMé) data, in parallel with c) metazoan sedaDNA occurrences (core PADMé). Pollinic data are presented in percentages (on total sum excluding *Alnus*, Cyperaceae and aquatic taxa). Plant sedaDNA taxa are presented as counts relative to the total assigned reads for Viridiplantae. Taxa comprising less than 0.1% reads assigned to Viridiplantae (Group B, Fig. 7a) are depicted with pale color bars. Blue bands: marine influence (i.e., synchronous increase of CaCO3%, Ca/Ti-XRF ratio and marine bio-indicators percentages) in the ANE-C3 core. Yellow bands: peaty deposits in PADMé and/or ANE-C3 cores. Solid dark lines delimit the main palynozones. Limits A to C indicate the main anthropic thresholds.

5.1. Environmental dynamics

5.1.1. An alluvial plain in the Kerallé valley: estuarine facies and peat deposits

Between 7.3 and 7 cal ka BP, marine biogenic production (i.e., $CaCO_3$%, Ca/Ti-XRF ratio and marine palynological bio-indicators) is recorded in core ANE-C3, which agree with the maximum percentages of Amaranthaceae, a taxon associated with salt marshes in coastal environments (first blue band and blue curve in Fig. 10a and b). The combination of these proxies reveals the proximity of marine influence in a coastal plain-like system, close to the coring site. This interval, in contact with the bedrock, is characterized by high sedimentation rates (Fig. 2a) and corresponds to the initial flooding of the Kerallé valley in a context of rapid RSL rise (García-Artola et al., 2018), leading to the establishment of the Transgressive System Tract (TST) in the central part of the valley (Gorczyńska, 2022). This led to the spreading out of a floodplain and gradual infilling of the valley by fine-grained deposits (Fig. 2b). This Mesolithic interval is also marked, at a more regional scale, by high arboreal taxa percentages (Fig. 10b), reflecting regionally well-developed tree cover, as largely observed in Brittany at that time (e.g., Marguerie, 1992; David, 2014; van Beek et al.,2018).

Between 7 and 6.4 cal ka BP, in the ANE-C3 core, marine proxies (i.e., $CaCO_3$%, Ca/Ti-XRF ratio and marine palynological bio-indicators) decrease synchronously with an increase in TOC values testifying to a peat deposit, as also attested in the PADMé core (Fig. 2b and 3b). The weaker marine influence in the upstream part of the Kerallé valley could have been induced by the development of a paleo-coastal barrier in the downstream part, leading to the gradual closure of the system (Gorczyńska, 2022). Moreover, this shift occurred synchronously with the slowing down of the RSL rise recorded along Brittany coasts from ~7 to 6 cal ka BP (Goslin et al., 2015; Stéphan et al., 2015; García-Artola et al., 2018). This led to a sediment accumulation in sheltered bays and estuarine systems, promoting the progressive disconnection of the upstream system from marine influence (e.g., Stéphan, 2019). The Kerallé valley was therefore gradually infilled, resulting in the elevation of the system that became disconnected from the tidal incursion, as is currently observed in the estuarine system (Dalrymple et al., 1992; Fletcher III et al., 1993). This led to the progressive development of freshwater marshes close to the coring site, as synchronously recorded in the PADMé core by the sedaDNA occurrences of Poaceae (especially *Phragmites*) together with aquatic taxa (*Callitriche* and Cyperaceae) between 7 and 6.6 cal ka BP (S1 in Fig. 10b), while between 6.6 and 6.4 cal ka BP, sedaDNA occurrences of arboreal taxa suggest the closure of the system (S2 in Fig. 10b).

Between 6.4 and 6 cal ka BP, a new occurrence of estuarine facies is recorded in core ANE-C3 (second blue band in Fig. 10a). This interval contains dinocysts taxa and infralittoral foraminiferal species (Gorczyńska, 2022), as well as increases in Amaranthaceae percentages (i.e., salt marsh plants), indicating a growing tidal influence. The return of the estuarine facies in the Kerallé valley suggests the destabilization of the paleo-coastal barrier and/or marine incursions in the upstream part of the valley also detected by Gorczyńska (2022). This interval coincides with stormy events already recorded along the Brittany coast (van Vliet-Lanoë et al., 2014) and northern European coast (Normandy: Sorrel et al., 2009/Denmark: Goslin et al., 2018). According to sedaDNA data, the presence of Poaceae (and especially *Phragmites*) likely signals a re-opening of the landscape at 6.4 cal ka BP (pink/blue bars in Fig. 10b), while these taxa then being able to develop in former subhalophilous meadows (Quéré et al., 2008).

5.1.2. The continentalization of the Kerallé valley

From 6 cal ka BP, the system closed again. In the PADMé core, sedaDNA data suggest a high arboreal signal from 6 cal ka BP interrupted, between 5.6 and 5.4 cal ka BP, by a re-increase of the herbaceous signal (i.e., Poaceae and Cyperaceae). At 6 cal ka BP, marine bio-indicators as well as Amaranthaceae pollen grains recorded in core ANE-C3 become scarce, especially from 5.4 cal ka BP (Fig. 10a and b). At that time, the peaty deposit reflects a major shift in environmental dynamics in the Kerallé valley, from an estuarine influence during the 7.3–6 cal ka BP interval to a clearly established continental influence starting around 5.4 cal ka BP. The continental influence is then attested by the rise in arboreal pollen grains, which peak at that time. Interestingly, sedaDNA data show a concordant pattern of vegetation (i.e., highest occurrences of trees) after 5.4 cal ka BP (Fig. 10b). Both proxies argue for a surrounding landscape covered by woodland, probably occupying the drained slopes of the watersheds (*Corylus, Alnus*, and to a less extent *Quercus*, the last of which may reflect a distant vegetation signal). *Fagus*, *Betula*, *Carpinus,* and Rosaceae appear to be present locally, as revealed by their occurrences in sedaDNA data (S6 in Fig. 8a), while the occurrences of *Hedera*, *Ulmus/Tilia* and *Ilex* pollen grains (palynozone P2c in Fig. 4c) reflect a more distal origin.

5.2. Anthropic dynamics

To discuss anthropic dynamics, specific taxa were selected from both palynological and sedaDNA datasets (Fig. 10b). First, it is important to consider that, among the main pollen taxa, the total arboreal signal (mainly represented by *Corylus*) and the herbaceous signal (mainly represented by Poaceae) are anti-correlated through time when plotted as percentages, highlighting landscape closure and opening, respectively. Second, human activities can be discussed through the development of Anthropogenic Indicators (AI), such as the sum of ruderal and arable weed pollen taxa and the sedaDNA record of the Urticaceae (red curve/bars in (Fig. 10b). Finally, pastoral activities can be detected through the development of Pastoral Indicators (PI) represented by Asteraceae (i.e., Asteroideae, Cichorioideae) and *Plantago lanceolata* pollen taxa (orange curves in Fig. 10b) according to the literature and modern calibration of the anthropogenic pollen signal at Plouescat (Data in Brief, David et al., *submitted*). In the sedaDNA data, Asteraceae and Plantaginaceae (including indeterminate species, *Plantago* spp. and *Digitalis*) represent PI. Furthermore, to discuss pastoral activities, the metazoan occurring at least once in the PADMé sequence with more than 5 assigned reads (i.e., *Bos* spp., Caprinae comprising *Ovis* and indeterminate Caprinae, and *Canis* spp.) are shown in Fig. 10c. However, while it is well established that the *Ovis* genus did not originate from western Europe and is therefore necessarily domestic in our study (Ureña et al., 2018; Her et al., 2022), this is not the case for the *Bos* genus, for which wild representatives are known to have been present in Brittany (Upadhyay et al., 2017). As it was not possible to identify the *Bos* species in our study, their wild or domestic status remains uncertain.

5.2.1. Mesolithic to the late Neolithic period (~7.3–4.5 cal ka BP): scarce human evidence

Until 4.5 cal ka BP, the progressive infilling of the Kerallé valley led to the progradation of continental environments, and the ancient coastal plain became gradually colonized by arboreal taxa. Although, anthropogenic influence is not obvious, even if weak *Cerealia*-type occurrences can be seen between 6.8 and 4.5 cal ka BP (red dots in Fig. 10b). It is worth noting that the identification of *Cerealia*-type pollen grains is based on size criteria (i.e., grain diameter of 47 μm and annulus diameter of 11 μm; Joly et al., 2007). However, size criteria are now controversial in the light of recent studies conducted on modern plants that reveal some examples of wild littoral grasses reaching equivalent morphometric values (Lambert et al.,2024). Considering the close proximity of a salt marsh to the studied coring site until 5.4 cal ka BP and in the absence of other clear AI or PI, these large Poaceae grains could be associated with either natural littoral grasses or an extremely weak anthropogenic signal. Furthermore, arboreal pollen grains are well represented up to 4.5 cal ka BP, reflecting a wooded landscape at the regional scale, while sedaDNA data reflect an open surrounding landscape dominated by herbaceous taxa up to 5.4 cal ka BP. The Poaceae signal exhibits recurrent peaks in both pollen and sedaDNA records,

from the Early to Recent Neolithic (i.e., ~7–5.4 ka BP; Fig. 10b). Incursions in the pollen curve may be attributed to an increase in *Phragmites*, as revealed by sedaDNA data, but the low taxonomic resolution does not allow this specific taxon to be distinguished. The concomitant signal between these two proxies supports a local origin of Poaceae, consistent with the proximity of salt marshes or subhalophilous meadows described above (see section 5.1.1).

Human presence could also be demonstrated all along the core by the presence of *Canis* spp. sedaDNA, including sequences that are possibly dog. Regarding pastoral activities, the first occurrences of mammals associated with these practices are evident since the early Neolithic, around 6.7 cal ka BP, with evidence of Caprinae (among which *Ovis* spp.), while the domestic/wild status of *Bos* could not be determined (Upadhyay et al., 2017; Ureña et al., 2018; Her et al., 2022).

Despite the high concentration of gallery graves recorded around the Bay of Goulven (LeCerf, 1985; Sparfel et al., 2004; Gorczyńska et al., 2023b) and traces of domestic mammal sedaDNA, neither pollinic nor plant sedaDNA data reflect a pronounced anthropic influence during the recent Neolithic or beginning of the late Neolithic. This could be explained by the core retrieval location, which is further upstream than the coastal area where archaeological evidence of human activities is concentrated. Following this hypothesis, our results reflect a limited occupation of the territory, confined to areas near the shore during this period. Furthermore, in the British Isles, the nature of Neolithic subsistence, particularly the importance of cereal farming, are debated (Thomas, 1999; Rowley-Conwy, 2004; Stevens and Fuller, 2012). Despite the status of the agricultural revolution (e.g., Childe, 1952), the change in livelihood mode does not seem to be constant across the Neolithic period. Some studies argue for less reliance on cereals, in favor of pastoralism, alongside continued exploitation of natural resources (hunting, fishing, and gathering) during the late Neolithic at the scale of the British Isles (Entwhislte and Grant, 1989; Thomas, 1999; Stevens and Fuller, 2012).

In this interval, Juglandaceae taxa, of which *Juglans* is the only representative of the family in Europe, occur in sedaDNA data from the PADMé core (Fig. 8a) but not in pollinic analyses from the ANE-C3 core. It should be noted that no reads of *Juglans* were identified in any of the control. Although, it was long considered to have been introduced by Gallo-Roman farmers (Beug, 1975; Visset, 1979, 1989), *Juglans* occurrences have also been reported in palynological records from the southern part of the Armorican domain at the end of the Mesolithic (Visset et al., 2004; Joly and Visset, 2005, 2009) and during the Neolithic (Visset et al., 1996; Cyprien, 2001; Ouguerram, 2002), Bronze Age (Visset et al., 1995) and second Iron Age (Marguerie, 1992) periods. In our study, traces of Juglandaceae are detected in the sedaDNA record from the Mesolithic, and more intensively during the Neolithic (5.8 and 4.7–4.2 cal ka BP) and Iron Age (2.6–2.1 cal ka BP; Fig. 8a). These occurrences could correspond to walnuts or timber goods on the studied site, likely brought by human populations from other areas. This would imply exchanges with southern localities and probably with Mediterranean or Eastern European regions where walnut trees were established (Pollegioni et al. 2017, 2020; Krebs et al. 2022). Another hypothesis is based on well-established exchanges with the Iberian Peninsula (Pailler, 2009, 2012; Nicolas et al., 2013; Nicolas, 2016a) where *Juglans* was attested during the Neolithic (Lopez-Garcia and Lopez-Saez, 2000). However, the highest occurrences of *Juglans* are synchronous with a forest recovery, and more particularly to maximum assigned reads corresponding to Rosaceae (i.e., *Prunus* and *Malus;* Fig. 8a), raising the question of the natural development of this anemophilous species in the Kerallé valley. Thus, the absence of *Juglans* pollen from the fossil record could be due to the very low pollen production of this taxon at the limit of its geographical distribution.

5.2.2. *From the late Neolithic (~4.5 cal ka BP): a growing anthropogenic signal*

From 4.5 cal ka BP (i.e., limit A; Fig. 10), the arboreal signal drops, while Poaceae, arable weeds, and ruderal taxa gradually increase, all which suggest the beginning of landscape clearing due to human deforestation. This evidence is consistent with the substantial number of reads attributed to *Bos* and *Ovis* spp. in the sedaDNA data around 4.6–4.4 cal ka BP, attesting to a greater number of animals linked with anthropic activities. Regarding the number of reads (more than 20) and the association with another domesticated mammal (i.e., *Ovis*) we could hypothesize that, at this time, some of the *Bos* spp. detected could be domestic. This late Neolithic anthropogenic signal is in line with archaeological evidence of Bell Beaker culture, the first metal-working society in north-western Europe, which settled in Plouescat at that time (Nicolas et al., 2015).

From 4 cal ka BP (i.e., limit B; Fig. 10), at the onset of the Bronze Age, a major shift is recorded in the pollinic data marked by a strong landscape opening accompanied by higher pollen diversity corresponding to an increase in herbaceous taxa (Fig. 4b and c). This anthropogenic pollen signal is consistent with local archaeological evidence (Briard et al., 1970) and other paleobotanical observations made in northern Brittany (e.g., Morzadec-Kerfourn, 1974; David, 2014; Fernane et al., 2014). These data suggest an intensification of agropastoral practices consistent locally and regionally with the wider land use suggested by grave distribution (Nicolas and Pailler, 2018) and the development of the first field system by ~4 ka BP (Blanchet et al., 2019). Unfortunately, during the Bronze Age interval (i.e., ~4.2–2.7 ka BP), few aDNA sequences were assigned to Viridiplantea (<0.1%) or Metazoa (Fig. 6a and 7), thus biasing the related sedaDNA interpretation (Pedersen et al., 2016). A previous palynological study carried out on a shorter temporal sequence from the Porsguen peat bog (i.e., late Neolithic–middle Bronze Age), highlighted the same dynamic, with a first phase of clearing by fire at the end of the Neolithic, followed by grazing and then cultivation (Briard et al., 1970; Morzadec-Kerfourn, 1969, 1974). In this peat bog sequence, a more intense phase of anthropization was identified during the early Bronze Age, marked by the deforestation and the development of agro-pastoral practices attested by *Cerealia*-type occurrences (Morzadec-Kerfourn, 1969, 1974) and bones of domesticated mammals (i.e., *Equus asinus, Ovis aries and Bos* spp.; Briard et al., 1970). In core ANE-C3, the middle Bronze Age period is marked by increased anthropic influence, as shown by a new step in arboreal pollen decline and by *Cerealia*-type occurrences, while ruderal and arable weed taxa as well as PI percentages (i.e., Asteroideae, *Plantago lanceolata*) remain constant from the late Neolithic (Fig. 10b).

Finally, at 2.7 cal ka BP, corresponding to the beginning of the Iron Age (i.e., limit C; Fig. 10), a third anthropic threshold is marked by a drop in the arboreal pollen signal allowing Poaceae signal to develop. This could correspond to a new phase of landscape opening at the scale of the Kerallé watershed, or, more generally, at the regional scale. Indeed, the lower detection of Poaceae DNA in sediments, compared with what was previously observed in the lower part of the sequence, suggests a distal origin of these pollen grains, probably transported by the Kerallé River. Furthermore, ruderal and arable weed taxa and PI increase, while *Cerealia*-type pollen grains reach their highest occurrences. This trend is synchronous with the pastoral sedaDNA signal that re-increases at 2.6 cal ka BP (Fig. 10c) accompanied by *Bos* spp., Caprinae and *Canis* spp. occurrences. At the same time, the increase in detrital input (decreasing Ca/Ti-XRF ratio at 2.9 cal ka BP; Fig. 10a) can likely be attributed to human-induced soil erosion driven by the major forest cover reduction in the Kerallé watershed, in a context of intensification of agropastoral activities and metallurgical practices. Since 2.4 cal ka BP (i.e., the Second Iron Age), both arboreal taxa and the pollinic signal of pastoralism (i.e., PI; Fig. 10b) rise, suggesting the predominance of agropastoral activities, in the vicinity of the studied site. In parallel, the sedaDNA data indicates significant occurrences of domestic mammals (Fig. 10c) and anthropogenic indicators (e.g., Urticaceae, Asteraceae and Plantaginaceae; Fig. 10b) at 2.6, 2.2 and 2.1 cal ka BP. During the Roman period, the pollinic record shows little variation while the preservation of sedaDNA is poor, with few reads assigned to

Viridiplantea (<0.1%) or Metazoa.

5.2.3. Anthropic dynamics in Plouescat compared with regional thresholds

While environmental dynamics could explain the weak anthropogenic signal in the upstream part of the Kerallé valley during most of the Neolithic (see section 5.1), a similar observation can also be made about Brittany at the regional scale (van Beek et al., 2018; Penaud et al., 2020; David et al., 2022). An increase in the anthropogenic pollen signal during the Early Neolithic has been reported at certain localities in southern Brittany (Guidel: Fernane et al., 2015/Kerpenhir: Visset et al., 1996; Suscinio: Visset and Bernard, 2006) coinciding with the arrival of the first farmers in Brittany (i.e., Linear Pottery Culture; Blanchet et al., 2010) and inducing an anthropogenic pollen signal at the local scale.

At the scale of Brittany, the Bronze Age (from ~4.2 ka BP) appears as a main anthropic threshold, marked by the progressive decline of arboreal taxa consistent with the rise of Poaceae and anthropogenic pollen indicators (north Brittany: this study; west Brittany: Fernane et al., 2014; Valero et al., 2023; south Brittany: Fernane et al., 2015; David et al., 2022; regional compilation: van Beek et al., 2018). This is consistent with the archaeological context of metalwork development and demographic growth (Briard, 1965; Mohen and Olivier, 1989; Nicolas, 2011). The 4.2 ka BP limit also corresponds to a climatic threshold, leading to the intensification of a winter precipitation regime over northern Europe, that seems to have enhanced the transmission of the anthropogenic pollen indicators (otherwise more developed) into sediment from watershed to coastal areas (Penaud et al., 2020; David et al., 2022). Considering records with comparable geomorphological and sedimentary contexts, a shift in anthropic threshold between northern (Plouescat, 4.5–4 cal ka BP: this study) and southern (Guidel, 3.7 cal ka BP: Fernane et al., 2015; see David et al., 2022 for a revision of the age model) localities is observed. The earlier anthropogenic signal in Plouescat could be the result of a greater human concentration in the nearby area (i.e., settlement of the Bell Beaker Culture), which could be due to a local particularity or be the result of cumulative uncertainties in the radiocarbon dating of the compared records.

Finally, the Iron Age appears as a second threshold of anthropization in Brittany, marked by a sharp decrease in arboreal signal and the upsurge of AI and PI. This threshold is detected at around 2.7 cal ka BP (i.e., first Iron Age) in Plouescat and at around 2.4 cal ka BP (i.e., second Iron Age) at the macro-regional scale of southern Brittany (Guidel: Fernane et al., 2015/south-Armorican platform: Penaud et al., 2020; David et al., 2022). To explain these shifts in anthropic thresholds between the south and north Brittany coasts, new long temporal records must be acquired along the north coast to discriminate obvious differences from artefacts or uncertainties.

6. Conclusion

This study represents the first attempt to cross-correlate palynological (pollen) and sedimentary ancient DNA (sedaDNA) signals (plants and mammals) in a coastal/fluvial system in Brittany, here the Kerallé valley (northern Brittany, NW France), over the last 7.3 kyr BP. This multidisciplinary approach including sedimentological, palynological and paleogenomic analyses, allowed a robust paleoenvironmental reconstruction highlighting i) the sedimentological-geomorphological evolution of the upstream part of the Kerallé valley and ii) past vegetation cover dynamics. Between 7.3 and 6 cal ka BP, the study site evolved from a coastal plain subject to marine incursion, and then to a fluvial valley subject to detrital continental inputs, which increased from 5.4 cal ka BP.

Regarding anthropic dynamics, while archaeological data points to a limited human occupation along the coast at Plouescat during the middle and late Neolithic, a weak anthropogenic signal recorded in the upstream part of the Kerallé valley indicates a limited occupation of the territory, confined to areas near the shore. An unexpected record of *Juglans* in the sedaDNA dataset, never noticed before in pollen studies from this region, is difficult to interpret with our current understanding. In our study, the first evidence of anthropogenic pressure is found at 4.5 cal ka BP (i.e., end of the late Neolithic), corresponding to the Bell Beaker settlement (i.e., the first metallurgist community) attested in the vicinity of the studied site. The major anthropic threshold in pollinic data is recorded at 4 cal ka BP (i.e., the beginning of the Bronze Age) by clear signs of deforestation and through the rise of anthropogenic pollen indicators, while sedaDNA suffers from preservation biases throughout the Bronze Age period. Since 2.7 cal ka BP (i.e., first Iron Age), a third anthropic threshold is highlighted by both proxies, concomitant with occurrences of domesticated mammal sedaDNA, implying the intensification of local pastoral practices in a largely man-made environment.

This multidisciplinary study has enhanced our understanding of Holocene coastal environmental changes under both natural and anthropogenic forcings, and endorses the application of this methodology in other coastal sites. However, the sedaDNA conservation biases during the Bronze Age and Roman period, pose some limitations. To address this issue, an extensive analysis of the genomic data (including at the microbial level) is currently underway to gain a deeper understanding of past chemical and physical processes that occurred along the sequence with their related implications on sedaDNA results. Finally, the singularity of the anthropogenic imprint on the landscape in Plouescat compared with southern localities in Brittany needs to be confirmed by the investigation of new sequences.

Credit author statement

Details of individual contributions: David Ophélie (Conceptualization, Formal analysis, Investigation, Writing - original draft); Vidal Muriel (Project administration, Conceptualization, Formal analysis, Writing - original draft); Gorczyńska Aneta (Formal analysis, Investigation, Writing – review and editing); Penaud Aurélie (Writing – review and editing); Pailler Yvan (Writing – review and editing); Nicolas Clément (Writing – review and editing); Goubert Evelyne (Writing – review and editing); Stéphan Pierre (Project administration, Writing – review and editing); Ollivier Morgane (Formal analysis, Investigation, Writing - original draft); Barloy-Hubler Frédérique (Formal analysis, Investigation, Writing - original draft).

Declaration of competing interest

The authors declare that they have no known competing financial interests or personal relationships that could have appeared to influence the work reported in this paper.

Data availability

Supplementary data to this article will be available online in a Data In Brief paper.

Acknowledgments

This work is part of a PhD thesis (Ophélie David) financed by two Brittany Universities, UBS (Univ. Bretagne Sud) and UBO (Univ. Brest). It was also supported by the ISblue project, Interdisciplinary graduate school for the blue planet (ANR-17-EURE-0015) and co-funded by a grant from the French government under the program "*Investissements d'Avenir*" as part of the France 2030 investment plan.

For the cores discussed in this manuscript, we are indebted to the research projects involved in core retrieval and data acquisition: 1) ANE-C3 core: Labex-Mer "COCODILE" project (coord. P. Stéphan); 2) PADMé core: EUR-ISblue "PADMé" project (coord. M. Vidal). We thank Muriel Georget (EPOC; Univ. Bordeaux) for the ANE-C3 palynological treatments, as well as Nathan Martin and Regis Debruyne for their laboratory assistance with the sedaDNA study of the PADMé core. The bioinformatics analyses benefited from the Genouest service at the University of

Rennes. We also thank the Palgene platform and the Paleogenomics and Molecular Genetics Technical Platform of the MNHN (P2GM) at the "Musée de l'Homme", in Paris. Some dates were obtained thanks to the French ARTEMIS ^{14}C-AMS platform, and the others were acquired at the Beta Analytics Laboratory. The authors are grateful to the ZABrI ("*Zone Atelier Brest Iroise*", CNRS-INEE) for the funding of the dating and for fruitful interdisciplinary exchanges about human dynamics and Holocene paleoenvironments.

Finally, we would like to thank Helen McCombie from the *Bureau de Traduction de l'Université* (Translation Office) of the University of Brest for improving the English of this article.

Appendix A. Supplementary data

Raw data are available in a Zenodo repository: https://doi.org/10.5281/zenodo.12731174.

Supplementary data to this article will be available online in a Data In Brief paper.

References

Abgrall, C., 1919. Etablissement gallo-romain de Gorré-bloué en Plouescat. BSAF 16, 32–97.

Altschul, S.F., Gish, W., Miller, W., Myers, E.W., Lipman, D.J., 1990. Basic local alignment search tool. J. Mol. Biol. 215 (3), 403–410. https://doi.org/10.1016/S0022-2836(05)80360-2.

Bajard, M., Sabatier, P., David, F., Develle, A.L., Reyss, J.L., Fanget, B., Malet, E., Arnaud, D., Augustin, L., Crouzet, C., Poulenard, J., Arnaud, F., 2016. Erosion record in Lake La Thuile sediments (Prealps, France): evidence of montane landscape dynamics throughout the Holocene. Holocene 26 (3), 350–364. https://doi.org/10.1177/0959683615609750.

Ballèvre, M., Bosse, V., Dabard, M.P., Ducassou, C., Fourcade, S., Paquette, J.L., Peucat, J.J., Pitra, P., 2013. Histoire géologique du massif Armoricain: actualité de la recherche. Bull. Soc. Géol. Minér. Bretagne 500, 5–96. https://hal-insu.archives-ouvertes.fr/insu-00873116.

Baltzer, A., Cassen, S., Walter-Simonnet, A.V., Clouet, H., Lorin, A., Tessier, B., 2015. Variations du niveau marin Holocène en Baie de Quiberon (Bretagne sud): marqueurs archéologiques et sédimentologiques. Quaternaire 26 (2), 105–115. https://doi.org/10.4000/quaternaire.7201.

Battistini, R., 1953. Le littoral septentrional du Léon : principaux problèmes morphologiques. B.A.G.F. 30 (232), 58–71. https://doi.org/10.3406/bagf.1953.7410.

Battistini, R., 1955. Description du relief et des formations quaternaires du littoral breton entre Brignogan et Saint-Pol-de-Léon (Finistère). Bull. inf. (Com. Cent. Océanogr. Etud. Côtes) 7 (10), 468–491.

Battistini, R., Martin, S., 1956. La «Plate-forme à écueils» du Nord-Ouest de la Bretagne. Norois 10 (1), 147–161. https://doi.org/10.3406/noroi.1956.1121.

Behre, K.E., 1981. The interpretation of anthropogenic indicators in pollen diagrams. Pollen Spores 23, 225–244.

Behre, K.E. (Ed.), 1986. Anthropogenic Indicators in Pollen Diagrams. AA Balkema, Rotterdam, p. 232p.

Bennet, K.D., 1992. Psimpoll- quickbasic program that generates postscript page description of pollen diagrams. INQUA Commission for the Study of the Holocene: Working Group on Data-Handling Methods, Newsletter 8, 11–12.

Beug, H.-J., 1961. Beiträge Zur Postglazialen Floren- Und Vegetationsgeschichte in Süddalmatien: Der See „Malo Jezero" Auf Mljet: Teil I: Vegetationsentwicklung. Flora Oder Allg. Bot. Ztg. 150 (4), 600–631. https://doi.org/10.1016/S0367-1615(17)33232-9.

Beug, H.J., 1975. Man as a factor in the vegetational history of the Balkan peninsula. In: Jordanov, D., et al. (Eds.), Problem of Balkan Flora and Vegetation, Sofia, pp. 72–78.

Blaauw, M., Christen, J.A., 2011. Flexible paleoclimate age-depth models using an autoregressive gamma process. Bayesian Anal 6 (3), 457–474. https://doi.org/10.1214/11-BA618.

Blanchet, S., Forré, P., Fromont, N., Hamon, C., Hamon, G., 2010. Un habitat du Néolithique ancien à Betton «Pluvignon»(Ille-et-Vilaine). Présentation synthétique et premiers résultats. Premiers Néolithiques de l'Ouest. Cultures, réseaux, échanges des premières sociétés néolithiques à leur expansion. Presses Universitaires de France, Rennes, pp. 15–40.

Blanchet, S., Mélin, M., Nicolas, T., Pihuit, P., 2017. Le Bronze moyen et l'origine du Bronze final en Bretagne. In: Lachenal, T., Mordant, C., Nicolas, T., Véber, C. (Eds.), *Le Bronze moyen et l'origine du Bronze final en Europe occidentale (XVIIe-XIIIe siècle avant notre ère)*. Strasbourg, Assocation pour la Valorisation de l'Archéologie du Grand Est, vol. 1. Monographies d'Archéologie du Grand-Est, pp. 305–323.

Blanchet, S., Favrel, Q., Fily, M., Nicolas, C., Nicolas, T., Pailler, Y., Ripoche, J., 2019. Le Campaniforme et la genèse de l'âge du Bronze ancien en Bretagne : vers une nouvelle donne. In: Montoya, C., Fagnart, J.-P., Locht, et J.-L. (Eds.), *Préhistoire de l'Europe du Nord-Ouest : mobilité, climats et identités culturelles*, volume 3, Néolithique – âge du Bronze, Actes du XXVIIIe Congrès préhistorique de France, Amiens, 30 mai-4 juin 2016. Société préhistorique française, Paris, pp. 269–288.

Blott, S.J., Pye, K., 2001. GRADISTAT: a grain size distribution and statistics package for the analysis of unconsolidated sediments. Earth Surf. Process. Landforms 26, 1237–1248. https://doi.org/10.1002/esp.261.

Bond, G., Showers, W., Cheseby, M., Lotti, R., Almasi, P., deMenocal, P., Priore, P., Cullen, H., Hajdas, I., Bonani, G., 1997. A pervasive millenial-scale cycle in North Atlantic Holocene and glacial climates. Science 278, 1257–1266. https://doi.org/10.1126/science.278.5341.1257.

Bond, G., Kromer, B., Beer, J., Muscheler, R., Evans, M., Showers, W., Hoffmann, S., LottiBond, R., Hajdas, I., Bonani, G., 2001. Persistent solar influence on North Atlantic climate during the Holocene. Science 294, 2130–2136. https://doi.org/10.1126/science.1065680.

Bossard, S., 2015. Les souterrains et autres architectures enterrées de L'âge du Fer en Bretagne et Basse-Normandie. Analyse de structures de stockage spécifiques au nord-ouest de la Gaule (VIe - Ier siècle avant n. è.). Mémoire de master, Université de Nantes. 339p.

Briard, J., 1965. Les dépôts bretons et l'Age du Bronze atlantique, vol. 352p. Laboratoire d'Anthropologie préhistorique, Rennes.

Briard, J., Guerin, C., Morzadec-Kerfourn, M.-T., Plusquellec, Y., 1970. Le site de Porsguen en Plouescat (Finistère nord) : faune, flore, archéologie. Bull. Soc. Géol. Minér. Bretagne, II 2, 45–60.

Briard, J., 1984. Les tumulus d'Armorique, L'âge du Bronze en France. Picard, Paris, p. 304p.

Brisset, E., Miramont, C., Guiter, F., Anthony, E.J., Tachikawa, K., Poulenard, J., Arnaud, F., Delhom, C., Meunier, J.D., Bard, E., Suméra, F., 2013. Non-reversible geosystem destabilisation at 4200 cal. BP: sedimentological, geochemical and botanical markers of soil erosion recorded in a Mediterranean alpine lake. Holocene 23 (12), 1863–1874. https://doi.org/10.1177/0959683613508158.

Brooks, A., Edwards, R., 2006. The development of a sea-level database for Ireland. Ir. J. Earth Sci. 24 (1), 13–27. https://www.muse.jhu.edu/article/810049.

Brun, C., 2011. Anthropogenic indicators in pollen diagrams in eastern France: a critical review. Veg. Hist. Archaeobotany 20 (2), 135–142. https://doi.org/10.1007/s00334-010-0277-8.

Capo, E., Giguet-Covex, C., Rouillard, A., Nota, K., Heintzman, P.D., Vuillemin, A., et al., 2021. Lake sedimentary DNA research on past terrestrial and aquatic biodiversity: overview and recommendations. Quaternary 4 (1), 6. https://doi.org/10.3390/quat4010006.

Carpenter, M.L., Buenrostro, J.D., Valdiosera, C., Schroeder, H., Allentoft, M.E., Sikora, M., et al., 2013. Pulling out the 1%: whole-genome capture for the targeted enrichment of ancient DNA sequencing libraries. Am. J. Hum. Genet. 93 (5), 852–864.

Cassen, S., Audren, C., Hinguant, S., Lannuzel, G., Marchand, G., 1998. L'habitat Villeneuve-Saint-Germain du Haut-Mée (Saint-Étienne-en-Coglès, Ille-et-Vilaine). BSPF 95 (1), 41–75.

Chen, S., Zhou, Y., Chen, Y., Gu, J., 2018. fastp: an ultra-fast all-in-one FASTQ preprocessor. Bioinformatics 34 (17), i884–i890. https://doi.org/10.1093/bioinformatics/bty560.

Childe, V.G., 1952. Prehistoric communities of the British Isles. London.

Croudace, I.W., Rothwell, R.G. (Eds.), 2015. Micro-XRF Studies of Sediment Cores: Applications of a Non-destructive Tool for the Environmental Sciences, vol. 17. Springer, p. 668p.

Cyprien, A.L., 2001. Chronologie de l'interaction de l'homme et du milieu dans l'espace central et aval de la Loire. Thèse de Doctorat, Université de Nantes, Groupe d'Etude des Milieux Naturels. Nantes.

Dabney, J., Knapp, M., Glocke, I., Gansauge, M.T., Weihmann, A., Nickel, B., Valdiosera, C., Gracia, N., Pääbo, S., Arsuaga, J.L., Meyer, M., 2013. Complete mitochondrial genome sequence of a Middle Pleistocene cave bear reconstructed from ultrashort DNA fragments. Proc. Natl. Acad. Sci. USA 110 (39), 15758–15763. https://doi.org/10.1073/pnas.1314445110.

Daire, M.Y., Le Bihan, J.-P., Lorho, T., Quesnel, L., with the collaboration of, Baudry, A., Choisy, Guillou, Dréano, Y., Dupont, C., Gehres, B., Langouët, L., Mougne, C., 2015. Les modes d'occupation du littoral de la Bretagne continentale à l'âge du Fer. Une première approche. In: Olmer, F., Roure, R. (Eds.), Les Gaulois au fil de l'eau, Actes du 37e colloque international de l'AFEAF, 8-11 mai 2013, Montpellier – France, Vol. 1. Communications, Bordeaux, Ausonius éditions, Mémoires, vol. 39, pp. 143–166.

Dalrymple, R.W., Zaitlin, B.A., Boyd, R., 1992. Estuarine facies models; conceptual basis and stratigraphic implications. J. Sediment. Res. 62 (6), 1130–1146. https://doi.org/10.1306/D4267A69-2B26-11D7-8648000102C1865D.

David, O., Penaud, A., Vidal, M., Fersi, W., Lambert, C., Goubert, E., Herlédan, M., Stéphan, P., Pailler, Y., Bourillet, J.F., Baltzer, A., 2022. Sedimentological and palynological records since 10 ka BP along a proximal-distal gradient on the Armorican shelf (NW France). Quat. Sci. Rev. 293, 107678. https://doi.org/10.1016/j.quascirev.2022.107678.

David, O., Vidal, M., Gorczyńska, A., Penaud, A., Pailler, Y., Nicolas, C., Debruyne, R., Martin, N., Goor, M., Garcia-Ladieu, P., Goubert, E., Stéphan, P., Ollivier, M., Barloy-Hubler, F., n.d. New Coastal Records in Northern Brittany (Plouescat, NW France): Sedimentological, Palynological and Paleogenomic Data over the Last 7.3. Ka BP (Submitted.

David, R., 2014. *Modélisation de la végétation holocène du Nord-Ouest de la France : Reconstruction de la chronologie et de l'évolution du couvert végétal du Bassin parisien et du Massif armoricain*. Thèse doctorat. Université de Rennes I, 284p. https://theses.hal.science/tel-01060260/.

Del Campo, J., Sieracki, M.E., Molestina, R., Keeling, P., Massana, R., Ruiz-Trillo, I., 2014. The others: our biased perspective of eukaryotic genomes. Trends Ecol. Evol. 29 (5), 252–259. https://doi.org/10.1016/j.tree.2014.03.006.

de Vernal, A., Henry, M., Bilodeau, G., 1999. Technique de préparation et d'analyse en micropaléontologie. Les Cahiers du GEOTOP 3. Université du Québec à Montréal, Montréal, Canada.
Devoir, A., 1912. Temoins mégalithiques des variations des lignes des rivages armoricains. BSAF 39, 220–239. https://gallica.bnf.fr/ark:/12148/bpt6k2077040/f290.item.
Durand, M., Mojtahid, M., Maillet, G.M., Baltzer, A., Schmidt, S., Blet, S., Marchès, E., Howa, H., 2018. Late Holocene record from a Loire River incised paleovalley (French inner continental shelf): insights into regional and global forcing factors. Palaeogeogr. Palaeoclimatol. Palaeoecol. 511, 12–28. https://doi.org/10.1016/j.palaeo.2018.06.035.
Entwhislte, R., Grant, A., 1989. The evidence for cereal cultivation and animal husbandry in the southern British Neolithic and Bronze Age. BAR. International Series 496, 203–215.
Fernane, A., Gandouin, E., Penaud, A., Van Vliet-Lanoë, B., Goslin, J., Vidal, M., Delacourt, C., 2014. Coastal palaeoenvironmental record of the last 7 ka BP in NW France: sub-millenary climatic and anthropic Holocene signals. Holocene 24, 1785–1797, 10.1177%2F0959683614551223.
Fernane, A., Pénaud, A., Gandouin, E., Goslin, J., van Vliet-Lanoë, B., Vidal, M., 2015. Climate variability and storm impacts as major drivers for human coastal marsh withdrawal over the Neolithic period (Southern Brittany, NW France). Palaeogeogr. Palaeoclimatol. Palaeoecol. 435, 136–144. https://doi.org/10.1016/j.palaeo.2015.05.029.
Fletcher III, C.H., Van Pelt, J.E., Brush, G.S., Sherman, J., 1993. Tidal wetland record of Holocene sea-level movements and climate history. Palaeogeogr. Palaeoclimatol. Palaeoecol. 102 (3–4), 177–213. https://doi.org/10.1016/0031-0182(93)90067-S.
Florenzano, A., 2019. The history of pastoral activities in S Italy inferred from palynology: a long-term perspective to support biodiversity awareness. Sustainability 11 (2), 404. https://doi.org/10.3390/su11020404.
Gandini, C., 2022. Regard sur les campagnes chez les Osismes. Peuplement et activités dans le Léon et la vallée de l'Aulne du second âge du Fer à la fin de l'Antiquité. Ann. Normandie 72 (2), 107–147.
García-Artola, A., Stéphan, P., Cearreta, A., Kopp, R.E., Khan, N.S., Horton, B.P., 2018. Holocene sea-level database from the Atlantic coast of Europe. Quat. Sci. Rev. 196, 177–192. https://doi.org/10.1016/j.quascirev.2018.07.031.
Gaudin, L., 2004. *Transformations spatio-temporelles de la végétation du nord-ouest de la France depuis la fin de la dernière glaciation. Reconstitutions paléo-paysagères.* Thèse doctorat. Université de Rennes I, 660p. https://tel.archives-ouvertes.fr/tel-00470150.
Giguet-Covex, C., Pansu, J., Arnaud, F., Rey, P.J., Griggo, C., Gielly, L., Domaizon, I., Coissac, E., David, F., Choler, P., Poulenard, J., Taberlet, P., 2014. Long livestock farming history and human landscape shaping revealed by lake sediment DNA. Nat. Commun. 5 (1), 3211. https://doi.org/10.1038/ncomms4211.
Giguet-Covex, C., Ficetola, G.F., Walsh, K., Poulenard, J., Bajard, M., Fouinat, L., Sabatier, P., Gielly, L., Messager, E., Develle, A.L., David, F., Taberlet, P., Brisset, E., Guiter, F., Sinet, R., Arnaud, F., 2019. New insights on lake sediment DNA from the catchment: importance of taphonomic and analytical issues on the record quality. Sci. Rep. 9, 14676. https://doi.org/10.1038/s41598-019-50339-1.
Giot, P.-R., L'Helgouach, J., Briard, J., Talec, L., Le Roux, C.T., Onnée, Y., Van Zeist, W., 1965. Le site du Curnic en Guissény (Finistère). Annales de Bretagne et des pays de l'Ouest 72 (1), 49–70.
Giot, P.-R., Morzadec, H., 1992. Des dolmens à couloir au péril des mers actuelles. RAO 9 (1), 57–66. https://doi.org/10.3406/rao.1992.979.
Giot, P.-R., Briard, J., Pape, L., 1995. In: France, Ouest- (Ed.), Protohistoire de la Bretagne. Rennes, p. 422p.
Goslin, J., Vliet-Lanoë, B.V., Stéphan, P., Delacourt, C., Fernane, A., Gandouin, E., Hénaff, A., Penaud, A., Suanez, S., 2013. Holocene relative sea-level changes in western Brittany (France) between 7600 and 4000 cal. BP: reconstitution from basal-peat deposits. Geomorphol. Relief Process. Environ. 19 (4), 425–444. https://doi.org/10.4000/geomorphologie.10386.
Goslin, J., Van Vliet-Lanoë, B., Spada, G., Bradley, S., Tarasov, L., Neil, S., Suanez, S., 2015. A new Holocene relative sea-level curve for western Brittany (France): insights on Isostatic dynamics along the Atlantic coasts of north-western Europe. Quat. Sci. Rev. 129, 341–365 j.quascirev.2015.10.029.
Goslin, J., Fruergaard, M., Sander, L., Gałka, M., Menviel, L., Monkenbusch, J., Thibault, N., Clemmensen, L.B., 2018. Holocene centennial to millennial shifts in North-Atlantic storminess and ocean dynamics. Sci. Rep. 8, 12778. https://doi.org/10.1016/j.quascirev.2015.10.029.
Gorczyńska, A., 2022. *Changements paléogéographiques et vestiges archéologiques côtiers en Bretagne durant l'Holocène moyen et récent. Apports d'une approche pluridisciplinaire et multi-scalaire.* Thèse de Doctorat, Université de Bretagne Occidental, p. 372p.
Gorczyńska, A., Stéphan, P., Pailler, Y., Nicolas, C., Pénaud, A., David, O., Vidal, M., Le Gall, B., 2023a. Holocene evolution of coastal dunes in western France: regional reconstruction from archaeological and historical data. Aeolian Res 60, 100851. https://doi.org/10.1016/j.aeolia.2022.100851.
Gorczyńska, A., Le Gall, B., Stéphan, P., Pailler, Y., 2023b. An interdisciplinary approach to Late/Final Neolithic coastal gallery graves in Brittany, Western France: the 3D structure, origin of stone material, and paleoenvironmental setting of the Kernic and Lerret monuments. Geoarchaeology. https://doi.org/10.1002/gea.21970.
Green, B.M., Finn, K.J., Li, J.J., 2010. Loss of DNA replication control is a potent inducer of gene amplification. Science 329 (5994), 943–946. https://doi.org/10.1126/science.1190966.
Grimm, E.C., 1987. CONISS: a FORTRAN 77 program for stratigraphically constrained cluster analysis by the method of incremental sum of squares. Comput. Geosci. 13 (1), 13–35. https://doi.org/10.1016/0098-3004(87)90022-7.
Hallégouët, B., Talec, L., Giot, P.-R., 1971. Trouvailles néolithiques à Kerlouan (Finistère). Annales de Bretagne 78 (1), 7–12.
Hallégouët, B., Moign, A., 1976. Historique d'une évolution de littoral dunaire : la baie de Goulven (Finistère), interactions entre forces naturelles et interventions humaines. Penn. Bed (Brest) 10 (84), 263–276.
Hammer, Ø., Harper, D.A.T., Paul, D.R., 2001. Past: Paleontological statistics software package for education and data analysis. Palaeontol. Electron. 4 (1), 9p.
Hebsgaard, M.B., Gilbert, M.T.P., Arneborg, J., Heyn, P., Allentoft, M.E., Bunce, M., Munch, K., Schweger, C., Willerslev, E., 2009. 'The farm beneath the sand' – an archaeological case study on ancient 'dirt' DNA. Antiquity 83 (320), 430–444. https://doi.org/10.1017/S0003598X00098537.
Heiri, O., Lotter, A.F., Lemcke, G., 2001. Loss on ignition as a method for estimating organic and carbonate content in sediments: reproducibility and comparability of results. J. Paleolimnol. 25, 101–110. https://doi.org/10.1023/A:1008119611481.
Her, C., Rezaei, H.R., Hughes, S., Naderi, S., Duffraisse, M., Mashkour, M., Naghash, H. R., Bălăşescu, A., Luikart, G., Jordan, J., Özüt, D., Kence, A., Bruford, M.W., Tresset, A., Vigne, J.D., Taberlet, P., Hänni, C., Pompanon, F., 2022. Broad maternal geographic origin of domestic sheep in Anatolia and the Zagros. Anim. Genet. 53 (3), 452–459. https://doi.org/10.1111/age.13191.
Hjelle, K.L., 1999. Modern pollen assemblages from mown and grazed vegetation types in western Norway. Rev. Palaeobot. Palynol. 107 (1–2), 55–81. https://doi.org/10.1016/S0034-6667(99)00015-9.
Hudson, S.M., Pears, B., Jacques, D., Fonville, T., Hughes, P., Alsos, I., Snape, L., Lang, A., Brown, A., 2022. Life before Stonehenge: the hunter-gatherer occupation and environment of Blick Mead revealed by sedaDNA, pollen and spores. PLoS One 17 (4), e0266789. https://doi.org/10.1371/journal.pone.0266789.
Joly, C., Visset, L., 2005. Nouveaux éléments d'anthropisation sur le littoral vendéen dès la fin du Mésolithique. Comptes Rendus Palevol 4 (3), 285–293. https://doi.org/10.1016/j.crpv.2004.12.006.
Joly, C., Barillé, L., Barreau, M., Mancheron, A., Visset, L., 2007. Grain and annulus diameter as criteria for distinguishing pollen grains of cereals from wild grasses. Rev. Palaeobot. Palynol. 146 (1–4), 221–233.
Joly, C., Visset, L., 2009. Evolution of vegetation landscapes since the Late Mesolithic on the French West Atlantic coast. Rev. Paleobot. Palynol. 154 (1–4), 124–179. https://doi.org/10.1016/j.revpalbo.2008.12.011.
Jónsson, H., Ginolhac, A., Schubert, M., Johnson, P.L.F., Orlando, L., 2013. mapDamage2.0: fast approximate Bayesian estimates of ancient DNA damage parameters. Bioinformatics 29, 1682–1684. https://doi.org/10.1093/bioinformatics/btt193.
Juhel, L., Charraud, F., Forré, P., Fromont, N., Hamon, C., Le Maux, N., Meunier, K., Pailler, Y., Wiethold, J., avec la collaboration de Errera, M., Collado, E., Leblanc, P., Pétrequin, P., Pihuit, P., Rolet, J., Seignac, H., 2015. Bretagne, Côtes-d'Armor, Lannion, Kervouric, un habitat du Néolithique ancien. Rapport final d'opération, fouille archéologique, Inrap GO, SRA Bretagne 331p. http://bibliothequenumeriquesrabretagne.humanum.fr/files/original/0d614baff452ce7eb1aa9f503e80d30b10ffe11b.
Kircher, M., Sawyer, S., Meyer, M., 2012. Double indexing overcomes inaccuracies in multiplex sequencing on the Illumina platform. Nucleic Acids Res. 40 (1), e3. https://doi.org/10.1093/nar/gkr771 e3.
Krebs, P., Ulmke, F., Tinner, W., Conedera, M., 2022. The Roman legacy on European chestnut and walnut arboriculture. Environ. Achaeol 1–22. https://doi.org/10.1080/14614103.2022.2137648.
Lambeck, K., Smither, C., Johnston, P., 1998. Sea-level change, glacial rebound and mantle viscosity for northern Europe. Geophys. J. Int. 134 (1), 102–144. https://doi.org/10.1046/j.1365-246x.1998.00541.x.
Lambert, C., Vidal, M., Penaud, A., Combourieu-Nebout, N., Lebreton, V., Ragueneau, O., Gregoire, G., 2017. Modern palynological record in the Bay of Brest (NW France): signal calibration for palaeo-reconstructions. Rev. Palaeobot. Palynol. 244, 13–25. https://doi.org/10.1016/j.revpalbo.2017.04.005.
Lambert, C., Vidal, M., Penaud, A., Le Roy, P., Goubert, E., Pailler, Y., Stéphan, P., Ehrhold, A., 2019. Palaeoenvironmental reconstructions during the Meso- to Neolithic transition (9.2 – 5.3 cal ka BP) in Northwestern France: palynological evidences. Holocene 29, 380–402, 10.1177%2F0959683618816457.
Lambert, C., Gervois, A., Vidal, M., Lardjane, S., Barbier-Pain, D., 2024. Relevance of the pollen grain size criteria in palynology to identify cereals from wild grasses. *Conference Abstract, Medpalynos,* 17-19 Juillet 2024 Salamanca (Spain). AbsRef: 006.
Lecerf, 1983. Plouescat (Finistère), Prospection sur la commune. Rapport de fouilles archéologique. Service Régional de l'Archéologie, Rennes, p. 10p.
Lecerf, 1984. Seconde campagne de fouille de sauvetage sur l'allée couverte de Kernic en Plouescat (Finistère). Rapport de fouilles archéologique. Service Régional de l'Archéologie, Rennes, 10p.
Lecerf, Y., 1985. L'allée couverte du Kernic à Plouescat (Finistère). BSAF 114, 17–34.
Le Goff, J.C., Roué, D., 1991. Plouescat, le Frouden : un site lié à l'industrie du sel. Bulletin de l'A.M.A.R.A.I. 4, 53–54.
Le Goffic, M., 2002a. Les souterrains de l'Âge du Fer. In: Tanguy, B., Lagrée, M. (Eds.), Atlas d'Histoire de Bretagne. Éditions Skol Vreizh, Morlaix, pp. 4–35.
Le Goffic, M., 2002b. Les stèles de l'Âge du Fer. In: Tanguy, B., Lagrée, M. (Eds.), Atlas d'Histoire de Bretagne. Éditions Skol Vreizh, Morlaix, pp. 36–37.
Leorri, E., Cearreta, A., Milne, G., 2012a. Field observations and modelling of Holocene sea-level changes in the southern Bay of Biscay: implication for understanding current rates of relative sea-level change and vertical land motion along the Atlantic coast of SW Europe. Quat. Sci. Rev. 42, 59–73. https://doi.org/10.1016/j.quascirev.2012.03.014.
Leorri, E., Fatela, F., Drago, T., Bradley, S.L., Moreno, J., Cearreta, A., 2012b. Lateglacial and Holocene coastal evolution in the Minho estuary (N Portugal): implications for

understanding sea-level changes in Atlantic Iberia. Holocene 23, 353–363. https://doi.org/10.1177/0959683612460786.
Li, H., Durbin, R., 2009. Fast and accurate short read alignment with Burrows–Wheeler transform. Bioinformatics 25 (14), 1754–1760. https://doi.org/10.1093/bioinformatics/btp324.
Lopez-Garcia, P., Lopez-Saez, J.A., 2000. Le paysage et la phase épipaléolithique–mésolithique dans les pré-Pyrénées aragonaises et le bassin moyen de l'Èbre à partir de l'analyse palynologique, Les derniers chasseurs-cueilleurs d'Europe occidentale (13000–5500 av. J.-C.). In: *Actes du colloque international de Besançon 1998* (Doubs, France), pp. 59–69.
Marchand, G., 2021. Sentes et ravines des mondes mésolithiques : pour une perspective plus symétrique de la néolithisation atlantique. In: Fromont, N., Marchand, G., Forré, P. (Eds.), *Statut des objets, des lieux et des Hommes au Néolithique. Actes du 32e colloque interrégional sur le Néolithique*, Le Mans, pp. 27–42, 24-25 novembre 2017.
Marguerie, D., 1992. Évolution de la végétation sous l'impact humain en Armorique du Néolithique aux périodes historiques. Thèse de doctorat, Université de Rennes 1, Travaux du Laboratoire d'Anthropologie n°40, 313p.
Martin, M., 2011. Cutadapt removes adapter sequences from high-throughput sequencing reads. EMBnet.journal 17 (1), 10–12. https://doi.org/10.14806/ej.17.1.200.
Mayewski, P.A., Rohling, E.E., Curt Stager, J., Karlén, W., Maasch, K.A., David Meeker, L., Meyerson, E.A., Gasse, F., Van Kreveld, S., Holmgren, K., Lee-Thorp, J., Rosqvist, G., Rack, F., Staubwasse, M., Schneider, R.R., Steig, E.J., 2004. Holocene climate variability. Quat. Res. 62, 243–255. https://doi.org/10.1016/j.yqres.2004.07.001.
Mazier, F., Galop, D., Brun, C., Buttler, A., 2006. Modern pollen assemblages from grazed vegetation in the western Pyrenees, France: a numerical tool for more precise reconstruction of past cultural landscapes. Holocene 16 (1), 91–103. https://doi.org/10.1191/0959683606hl908.
Menez, S., 1977. Les crêtes successives dunifiées de type Darss de la côte sud-ouest de la baie de Goulven (Finistère). Norois 96, 593–599. https://doi.org/10.3406/noroi.1977.3668.
Menez, Y., Lorho, T., 2013. La Bretagne. In: Malrain, F., Blancquaert, G., Lorho, T. (Eds.), *L'habitat rural du second âge du Fer : rythmes de création et d'abandon au nord de la Loire*. Paris, vol. 7. Inrap et CNRS Editions (Recherches archéologiques, pp. 169–191.
Mensing, S.A., Tunno, I., Sagnotti, L., Florindo, F., Noble, P., Archer, C., Zimmerman, S., Pavon- Carrasco, F.J., Cifani, G., Passigli, S., Piovesan, G., 2015. 2700 years of Mediterranean environmental change in central Italy: a synthesis of sedimentary and cultural records to interpret past impacts of climate on society. Quat. Sci. Rev. 116, 72–94. https://doi.org/10.1016/j.quascirev.2015.03.022.
Messager, E., Giguet-Covex, C., Doyen, E., Etienne, D., Gielly, L., Sabatier, P., Banjan, M., Develle, A.L., Didier, J., Poulenard, J., Julien, A., Arnaud, F., 2022. Two millennia of complexity and variability in a Perialpine Socioecological System (Savoie, France): the contribution of palynology and sedaDNA analysis. Front. Ecol. Evol. 10, 866781. https://doi.org/10.3389/fevo.2022.866781.
Meyer, M., Kircher, M., 2010. Illumina sequencing library preparation for highly multiplexed target capture and sequencing. Cold Spring Harb. Protoc. 2010 (6), pdb–prot5448.
Mohen, J.-P., Olivier, L., 1989. Les premiers métallurgistes. In: *Archéologie de la France: 30 ans de découvertes* : exposition Galeries nationales du Grand Palais. Paris, Editions de la Réunion des Musées nationaux, pp. 198–200.
Morzadec-Kerfourn, M.-T., 1969. Variations de la ligne de rivage au cours du Post-glaciaire le long de la côte nord du Finistère. Analyses polliniques de tourbes et de dépôts organiques littoraux. Bulletin de l'AFEQ 6 (4), 285–318. https://doi.org/10.3406/quate.1969.1140.
Morzadec-Kerfourn, M.-T., 1974. Variations de la ligne de rivage armoricaine au Quaternaire : analyses polliniques de dépôts organiques littoraux, vol. 1. Thèse de doctorat, Université de Rennes, 208p.
Murchie, T.J., Kuch, M., Duggan, A.T., Ledger, M.L., Roche, K., Klunk, J., Karpinski, E., Hackenberger, D., Sadoway, T., MacPhee, R., Froese, D., Poinar, H., 2021. Optimizing extraction and targeted capture of ancient environmental DNA for reconstructing past environments using the PalaeoChip Arctic-1.0 bait-set. Quat. Res. 99, 305–328. https://doi.org/10.1017/qua.2020.59.
Naughton, F., Bourillet, J.-F., Sanchez Goni, M.F., Turon, J.-L., Jouanneau, J.-M., 2007. Long-term and millennial-scale climate variability in northwestern France during the last 8850 years. Holocene 17, 939–953. https://doi.org/10.1177/0959683607082410.
Nicolas, C., 2011. Artisanats spécialisés et inégalités sociales à l'aube de la métallurgie: les pointes de flèches de type armoricain dans le nord du Finistère. BSPF 93–125. http://www.jstor.org/stable/23242627.
Nicolas, C., 2016a. La fin d'un monde? La région de Carnac du Campaniforme à l'âge du Bronze ancien. Bull. mém. Soc. Polymath. Morbihan 36p. https://hal.science/hal-02883859.
Nicolas, C., 2016b. Flèches de pouvoir à l'aube de la métallurgie : de la Bretagne au Danemark (2500-1700 av. n. è.). Sidestone, Leiden, p. 947p.
Nicolas, C., Pailler, Y., 2018. Quel(s) modèle(s) de sociétés pour la culture des Tumulus armoricains. In: Blanchet, S., Nicolas, T., Quilliec, B., Roberts, et B. (Eds.), Les sociétés du Bronze ancien atlantique du XXIVe au XVIIe s. av. J.-C., Rennes, 7-10 novembre 2018, Bordeaux, Ausonius.
Nicolas, C., Favrel, Q., Rousseau, L., Ard, V., Blanchet, S., Donnart, K., Fromont, N., Manceau, L., Marcigny, C., Marticorena, P., Nicolas, T., Pailler, Y., Ripoche, J., 2019. The introduction of the Bell Beaker culture in Atlantic France: an overview of settlements. In: Gibson, A. (Ed.), *Bell Beaker Settlements in Europe. The Bell Beaker Phenomenon from a Domestic Perspective*. Prehistoric Society Research Paper 9. Oxbow Books, Oxford & Philadelphia, pp. 329–352.
Nicolas, E., Marchand, G., Hénaff, X., Juhel, L., Pailler, Y., Darboux, J.R., Errera, M., 2013. Le Néolithique ancien à l'ouest de la Bretagne: nouvelles découvertes à Pen Hoat Salaün (Pleuven, Finistère). L'Anthropologie 117 (2), 195–237. https://doi.org/10.1016/j.anthro.2013.02.002.
Nicolas, E., Brisotto, V., Laubaune-Jean, F., Nicolas, T., 2015. Des bâtiments de la transition entre le Néolithique final et l'âge du Bronze ancien Une nécropole du Bas-Empire. *Rapport final d'opération, fouille archéologique*. Inrap GO, SRA Bretagne 176p.
Orlando, L., Allaby, R., Skoglund, P., Der Sarkissian, C., Stockhammer, P.W., Ávila-Arcos, M.C., Fu, Q., Krause, J., Willerslev, E., Stone, A.C., Warinner, C., 2021. Ancient DNA analysis. Nat. Rev Methods Primers 1 (1), 14. https://doi.org/10.1038/s43586-020-00011-0.
Ouguerram, A., 2002. *Histoire de la vallée de l'Erdre (affluent de la Loire, Massif armoricain, France) de la fin du Tardiglaciaire aux époques actuelles*. Thèse de Doctorat, Université de Nantes, Groupe d'études des milieux naturels. Nantes.
Pailler, Y., 2007. Des dernières industries à trapèzes à l'affirmation du Néolithique en Bretagne (5500-3500 av. J.-C.). Oxford, Archaeopress (BAR, International Series 1648, 340p.
Pailler, Y., Marchand, G., Blanchet, S., Guyodo, J.-N., Hamon, G., 2008. Le Villeneuve-Saint-Germain dans la péninsule Armoricaine : les débuts d'une enquête. In: Burnez-Lanotte, L., Ilett et, M., Allard, P. (Eds.), *Fin des traditions danubiennes dans le Néolithique du Bassin parisien et de la Belgique (5100-4700 av. J.-C.)*. Autour des recherches de Claude Constantin, Paris. Société préhistorique française, pp. 91–111 (Mémoire, 44.
Pailler, Y., 2009. Produire des lames polies en contexte rituel, le matériel poli d'Er-Lannic (Arzon). In: Cassen, S. (Ed.), *Autour de la Table. Explorations archéologiques et discours savants sur des architectures néolithiques à Locmariaquer Morbihan (Table des Marchands et Grand Menhir)*. Université de Nantes LARA. Nantes, pp. 632–641.
Pailler, Y., 2012. L'exploitation des fibrolites en Bretagne et ses liens avec les productions alpines. In: Pétrequin, P., Cassen, S., Errera, M., Klassen, L., Sheridan, A., Pétrequin, A.M. (Eds.), Jade. Grandes haches alpines du Néolithique européen. Ve et IVe millénaires av. J.-C. Cahiers de la MSHE C.N. Ledoux, vol. 2. Presses Universitaires de Franche-Comté et Centre de Recherche Archéologique de la Vallée de l'Ain, tome, Besançon, pp. 1168–1193.
Parducci, L., Matetovici, I., Fontana, S.L., Bennett, K.D., Suyama, Y., Haile, J., Kjaer, K. H., Larsen, N.K., Drouzas, A.D., Willerslev, E., 2013. Molecular-and pollen-based vegetation analysis in lake sediments from central Scandinavia. Mol. Ecol. 22 (13), 3511–3524. https://doi.org/10.1111/mec.12298.
Parducci, L., Alsos, I.G., Unneberg, P., Pedersen, M.W., Han, L.U., Lammers, Y., Sakari Salonen, J., Väliranta, M., Slotte, T., Wohlfarth, B., 2019. Shotgun environmental DNA, pollen, and macrofossil analysis of lateglacial lake sediments from southern Sweden. Front. Ecol. Evol. 7, 189. https://doi.org/10.3389/fevo.2019.00189.
Pedersen, M.W., Ruter, A., Schweger, C., Friebe, H., Staff, R.A., Kjeldsen, K.K., Mendoza, M.L.Z., Beaudoin, A.B., Zutter, C., Larsen, N.K., Potter, B.A., Nielsen, R., Rainville, R.A., Orlando, L., Meltzer, D.J., Kjaer, K.H., Willerslev, E., 2016. Postglacial viability and colonization in North America's ice-free corridor. Nature 537 (7618), 45–49. https://doi.org/10.1038/nature19085.
Penaud, A., Ganne, A., Eynaud, F., Lambert, C., Coste, P.O., Herlédan, M., Vidal, M., Goslin, J., Stéphan, P., Charia, G., Pailler, Y., Durant, M., Zumaque, J., Mojtahid, M., 2020. Oceanic versus continental influences over the last 7 kyrs from a mid-shelf record in the northern Bay of Biscay (NE Atlantic). Quat. Sci. Rev. 229, 106135. https://doi.org/10.1016/j.quascirev.2019.106135.
Pollegioni, P., Woeste, K., Chiocchini, F., Del Lungo, S., Ciolfi, M., Olimpieri, I., Tortolano, V., Clark, J., Hemery, G.E., Mapelli, S., Malvolti, M.E., 2017. Rethinking the history of common walnut (Juglans regia L.) in Europe: its origins and human interactions. PLoS One 12 (3), e0172541. https://doi.org/10.1371/journal.pone.0172541.
Pollegioni, P., Lungo, S.D., Müller, R., Woeste, K.E., Chiocchini, F., Clark, J., Hemery, G. E., Mapelli, S., Villani, F., Malvolti, M.E., Mattioni, C., 2020. Biocultural diversity of common walnut (Juglans regia L.) and sweet chestnut (Castanea sativa Mill.) across Eurasia. Ecol. Evol. 10 (20), 11192–11216. https://doi.org/10.1002/ece3.6761.
Quéré, E., Magnanon, S., Ragot, R., Gager, L., Hardy, F., 2008. In: Siloë (Ed.), Atlas floristique de Bretagne: la flore du Finistère, p. 693.
Reille, M., 1995. Pollen et spores d'Europe et d'Afrique du Nord: supplement 1. Laboratoire de Botanique Historique et Palynologie, Marseille, p. 327p.
Reimer, P., Austin, W., Bard, E., Bayliss, A., et al., 2020. The IntCal20 northern hemisphere radiocarbon age calibration curve (0–55 cal kBP). Radiocarbon 62 (4), 725–757. https://doi.org/10.1017/RDC.2020.41.
Rivière, G., 2007. Atlas floristique de Bretagne : la flore du Morbihan. Siloë. 655p.
Rowley-Conwy, P., 2004. How the west was lost: a reconsideration of agricultural origins in Britain, Ireland, and Southern Scandinavia. Curr. Anthropol. 45 (S4), S83–S113.
Sorrel, P., Tessier, B., Demory, F., Delsinne, N., Mouazé, D., 2009. Evidence for millennial-scale climatic events in the sedimentary infilling of a macrotidal estuarine system, the Seine estuary (NW France). Quat. Sci. Rev. 28 (5–6), 499–516. https://doi.org/10.1016/j.quascirev.2008.11.009.
Sparfel, Y., 2002. Géographie des sites funéraires du Néolithique à l'Age du Bronze moyen. Les exemples du nord-ouest du Léon et du Pays Bigouden (Master's thesis). Université de Bretagne Occidentale, Brest.
Sparfel, Y., Leroux, V.-E., Pailler, Y., Boujot, C., Le Goffic, M., 2004. Inventaire des mégalithes du Néolithique à l'Age du bronze dans le Finistère. Service Régional de l'Archéologie, Bretagne 617p.
Sparfel, Y., Pailler, Y., 2009. Les Mégalithes de l'arrondissement de Brest. Centre Régional d'Archéologie d'Alet, Institut Culturel de Bretagne, p. 290.
Stéphan, P., Goslin, J., Pailler, Y., Manceau, R., Suanez, S., Van Vliet-Lanoë, B., Henaff, A., Delacourt, C., 2015. Holocene salt-marsh sedimentary infillings and relative sea-level changes in West Brittany (France) from foraminifera-based transfer functions. Boreas 44, 153–177. https://doi.org/10.1111/bor.12092.

Stéphan, P., Dodet, G., Tardieu, I., Suanez, S., David, L., 2018. Dynamique pluri-décennale du trait de côte en lien avec les variations des forçages météo-océaniques au nord de la Bretagne (baie de Goulven, France). Geomorphol. Relief Process. Environ. 24 (1), 79–102. https://doi.org/10.4000/geomorphologie.11908.

Stéphan, P., 2019. Évolutions morphologiques et indices d'occupation humaine au Pléistocène et à l'Holocène le long des côtes françaises de la Manche et de l'Atlantique. Les nouvelles de l'archéologie 156, 53–59. https://doi.org/10.4000/nda.6996.

Stevens, C.J., Fuller, D.Q., 2012. Did Neolithic farming fail? The case for a Bronze Age agricultural revolution in the British Isles. Antiquity 86 (333), 707–722. https://doi.org/10.1017/S0003598X00047864.

Stuiver, M., Reimer, P.J., 1993. Extended 14C database and revised CALIB radiocarbon calibration program. Radiocarbon 35, 215–230.

Thomas, J., 1999. Understanding the Neolithic. A Revised Second Edition of Rethinking the Neolithic. Routledge, London.

Tinévez, J.-Y., Hamon, G., Querré, G., Marchand, G., Pailler, Y., Darboux, J.-R., Donnart, K., Marcoux, N., Pustoc'h, F., Quesnel, L., Oberlin, C., avec la coll de Roy, E., Villard, J.-F., , et al.Nicolas, É., 2015. Les vestiges d'habitat du Néolithique ancien de Quimper, Kervouyec (Finistère). BSPF 112 (2), 269–316.

Upadhyay, M., Chen, W., Lenstra, J., Goderie, C.R.J., MacHug, D.E., Park, S.D.E., Magee, D.A., Matassino, D., Ciani, F., Megens, H.J., Arendonk, J.A.M., Groenen, M. A.M., European Cattle Genetic Diversity Consortium, Crooijmans, R.P.M.A., 2017. Genetic origin, admixture and population history of aurochs (Bos primigenius) and primitive European cattle. Heredity 118, 169–176. https://doi.org/10.1038/hdy.2016.79.

Ureña, I., Ersmark, E., Samaniego, J.A., Galindo-Pellicena, M.A., Crégut-Bonnoure, E., Bolívar, H., Gómez-Olivencia, A., Rios-Garaizar, J., Garate, D., Dalén, L., Arsuaga, J. L., Valdiosera, C.E., 2018. Unraveling the genetic history of the European wild goats. Quat. Sci. Rev. 185, 189–198. https://doi.org/10.1016/j.quascirev.2018.01.017.

Valero, C., Penaud, A., Lambert, C., Vidal, M., Nicolas, C., Stéphan, P., Pailler, Y., Ehrhold, A., 2023. Holocene paleoenvironmental reconstructions in the Bay of Brest. Conference Abstract, *28iè RST,* 30 Octobre-3 Novembre 2023, Rennes (France).

van Beek, R., Marguerie, D., Bruel, F., 2018. Land use, settlement, and plant diversity in Iron Age Northwest France. Holocene 28 (4), 513e528. https://doi.org/10.1177/0959683617735590.

van Vliet-Lanoë, B., Penaud, A., Hénaff, A., Delacourt, C., Fernane, A., Goslin, J., Hallégouët, B., Le Cornec, E., 2014. Middle-to late-Holocene storminess in Brittany (NW France): Part II–The chronology of events and climate forcing. Holocene 24 (4), 434–453. https://doi.org/10.1177/0959683613519688.

van Zeist, W., 1963. Recherches palynologiques en Bretagne occidentale. Norois 37 (1), 5–19.

Velsko, I.M., Frantz, L.A., Herbig, A., Larson, G., Warinner, C., 2018. Selection of appropriate metagenome taxonomic classifiers for ancient microbiome research. mSystems 3 (4), 10–1128. https://doi.org/10.1128/msystems.00080-18.

Villard-Le Tiec, A., 2011. Stèles armoricaines de l'âge du Fer et organisation de l'espace funéraire. Les exemples de Melgven et de Paule. DAM 34, 323–337.

Visset, L., 1979. Recherches palynologiques sur la végétation Pléistocène et Holocène de quelques sites du district phytogéographique de Basse-Loire. Bull. Soc. Sci. Nat. Ouest Fr. Nantes, 282p.

Visset, L., 1989. La tourbière de Landemarais en Parigné (Ille-et-Vilaine, France). Étude pollinique. *Lejeunia*. série 129, 1–26.

Visset, L., Sellier, D., L'Helgouach, J., 1995. Le paléoenvironnement de la région de Carnac. Sondage dans le marais de Kerdual, La Trinité-sur-Mer (Morbihan). RAO 12, 57–71. https://doi.org/10.3406/rao.1995.1025.

Visset, L., L'Helgouach, J., Bernard, J., 1996. La tourbière submergée de la pointe de Kerpenhir à Locmariaquer (Morbihan). Etude environnementale et mise en évidence de déforestations et de pratiques agricoles néolithiques. RAO 13, 79–87. https://doi.org/10.3406/rao.1996.1041.

Visset, L., Cyprien, A.L., Ouguerram, A., Barbier, D., Bernard, J., 2004. Les indices polliniques d'anthropisation précoce dans l'ouest de la France. Le cas de Cerealia, Fagopyrum et Juglans. In: Richard, H. (Ed.), *Néolithisation précoce. Premières traces d'anthropisation du couvert végétal à partir des données polliniques.* Annales Littéraires, 777, Série Environnement, sociétés et archéologie, vol. 7. Presses Universitaires Franc-Comtoises, Besançon, pp. 69–79.

Visset, L., Bernard, J., 2006. Evolution du littoral et du paysage, de la presqu'île de Rhuys à la rivière d'Etel (Massif armoricain – France), du Néolithique au Moyen Age. ArchéoSciences 30, 143–156. https://doi.org/10.4000/archeosciences.315.

Walker, M., Gibbard, P., Head, M.J., Berkelhammer, M., Björck, S., Cheng, H., Cwynar, L. C., Fisher, D., Gkinis, V., Long, A., Lowe, J., Newnham, R., Rasmussen, S.O., Weiss, H., 2019. Formal subdivision of the Holocene series/epoch: a summary. J. Geol. Soc. India 93, 135–141. https://doi.org/10.1007/s12594-019-1141-9.

Warinner, C., Herbig, A., Mann, A., Fellows Yates, J.A., Weiß, C.L., Burbano, H.A., Orlando, L., Krause, J., 2017. A robust framework for microbial archaeology. Annu. Rev. Genom. Hum. Genet. 18, 321–356. https://doi.org/10.1146/annurev-genom-091416-035526.

Wood, D.E., Salzberg, S.L., 2014. Kraken: ultrafast metagenomic sequence classification using exact alignments. Genome Biol. 15, R46. https://doi.org/10.1186/gb-2014-15-3-r46.

Yoni, C., Hallégouët, B., 1998. Extractions d'amendements marins et recul de la ligne de rivage en baie de Goulven (Finistère). Les paradoxes de la gestion d'un site. Norois 177, 63–73. https://doi.org/10.3406/noroi.1998.6850.